



# Chromatin Separation Regulators Predict the Prognosis and Immune Microenvironment Estimation in Lung Adenocarcinoma

Zhaoshui Li<sup>1,2</sup>, Zaiqi Ma<sup>2</sup>, Hong Xue<sup>3</sup>, Ruxin Shen<sup>1</sup>, Kun Qin<sup>1</sup>, Yu Zhang<sup>1</sup>, Xin Zheng<sup>4\*</sup> and Guodong Zhang<sup>5\*</sup>

<sup>1</sup>Qingdao Medical College, Qingdao University, Qingdao, China, <sup>2</sup>Cardiothoracic Surgery Department, Qingdao Hiser Hospital Affiliated to Qingdao University, Qingdao, China, <sup>3</sup>Heart Center Department, Qingdao Hiser Hospital Affiliated to Qingdao University, Qingdao, China, <sup>4</sup>Cancer Center Department, Qingdao Hiser Hospital Affiliated to Qingdao University, Qingdao, China, <sup>5</sup>Thoracic Surgery Department, Shandong Cancer Hospital Affiliated to Shandong First Medical University, Jinan, China

## OPEN ACCESS

### Edited by:

Katarzyna Leszczyńska,  
Nencki Institute of Experimental  
Biology (PAS), Poland

### Reviewed by:

Hiroshi Harada,  
Kyoto University, Japan  
Monica Olcina,  
University of Oxford, United Kingdom

### \*Correspondence:

Xin Zheng  
zhengxin66999@163.com  
Guodong Zhang  
guodongzhang2022@163.com

### Specialty section:

This article was submitted to  
Cancer Genetics and Oncogenomics,  
a section of the journal  
Frontiers in Genetics

**Received:** 11 April 2022

**Accepted:** 23 May 2022

**Published:** 08 July 2022

### Citation:

Li Z, Ma Z, Xue H, Shen R, Qin K,  
Zhang Y, Zheng X and Zhang G (2022)  
Chromatin Separation Regulators  
Predict the Prognosis and Immune  
Microenvironment Estimation in  
Lung Adenocarcinoma.  
Front. Genet. 13:917150.  
doi: 10.3389/fgene.2022.917150

**Background:** Abnormal chromosome segregation is identified to be a common hallmark of cancer. However, the specific predictive value of it in lung adenocarcinoma (LUAD) is unclear.

**Method:** The RNA sequencing and the clinical data of LUAD were acquired from The Cancer Genome Atlas (TCGA) database, and the prognosis-related genes were identified. The Kyoto Encyclopedia of Genes and Genomes (KEGG) and Gene Ontology (GO) were carried out for functional enrichment analysis of the prognosis genes. The independent prognosis signature was determined to construct the nomogram Cox model. Unsupervised clustering analysis was performed to identify the distinguishing clusters in LUAD-samples based on the expression of chromosome segregation regulators (CSRs). The differentially expressed genes (DEGs) and the enriched biological processes and pathways between different clusters were identified. The immune environment estimation, including immune cell infiltration, HLA family genes, immune checkpoint genes, and tumor immune dysfunction and exclusion (TIDE), was assessed between the clusters. The potential small-molecular chemotherapeutics for the individual treatments were predicted via the connectivity map (CMap) database.

**Results:** A total of 2,416 genes were determined as the prognosis-related genes in LUAD. Chromosome segregation is found to be the main bioprocess enriched by the prognostic genes. A total of 48 CSRs were found to be differentially expressed in LUAD samples and were correlated with the poor outcome in LUAD. Nine CSRs were identified as the independent prognostic signatures to construct the nomogram Cox model. The LUAD-samples were divided into two distinct clusters according to the expression of the 48 CSRs. Cell cycle and chromosome segregation regulated genes were enriched in cluster 1, while metabolism regulated genes were enriched in cluster 2. Patients in cluster 2 had a higher score of immune, stroma, and HLA family components, while those in cluster 1 had higher scores of TIDES and immune checkpoint genes. According to the hub genes highly

expressed in cluster 1, 74 small-molecular chemotherapeutics were predicted to be effective for the patients at high risk.

**Conclusion:** Our results indicate that the CSRs were correlated with the poor prognosis and the possible immunotherapy resistance in LUAD.

**Keywords:** lung adenocarcinoma, chromosome segregation regulators, prognostic signature, immune environment, bioinformatics

## INTRODUCTION

Lung cancer is a malignant tumor with the highest mortality rate in the world (Nooreldeen and Bach, 2021). Lung adenocarcinoma (LUAD) is now the most common histological subtype of primary lung cancer (Travis et al., 2011; Torre et al., 2016; Hutchinson et al., 2019), accounting for more than 40% of cases (Hutchinson et al., 2019). Improvements in multimodal treatment strategies (e.g., targeted therapy, radiotherapy, and immunotherapy) have markedly increased the overall survival (OS) of LUAD-patients in recent years (Moreira and Eng, 2014; Jin et al., 2020), quite a few patients eventually become resistant to these therapies, partly attributed to the malfunctioning of genes that regulate cardinal bioprocesses (Philpott et al., 2017). Thus, sufficient strategies are needed to predict prognosis and guide individual treatment in LUAD. The availability of public cohorts with RNA sequencing data and improved technology brought the opportunity to identify a more generalized prognostic signature for LUAD. For instance, an immune-related four-gene prognostic signature in LUAD was identified to regulate the innate immune response and to be a benefit for the prognosis prediction (Sun et al., 2020). Pyroptosis-related prognostic gene signature and metabolism-associated gene signature were also identified as a predictor of the prognosis in LUAD-patients (He et al., 2020; Lin et al., 2021). However, the novel biomarkers with guiding significance for therapy of LUAD still need to be explored.

Mitotic cell division is commonly thought to involve the equal distribution of duplicated genomes into the two daughter cells through appropriate chromosome segregation (Neumüller and Knoblich, 2009; Sarkar et al., 2021). Abnormal chromosome segregation at mitosis causes the aneuploidy of the daughter cells with an unequal distribution of chromosomes (Levine and Holland, 2018), this is one way by which neoplastic cells accumulate the many genetic abnormalities required for tumor development (Gisselsson, 2008; Naylor and van Deursen, 2016; Levine and Holland, 2018). Moreover, mitotic errors and aneuploidization are found during tumor evolution, and the extent of chromosomal aberrations is correlated with tumor grade and poor prognosis (Loeper et al., 2001; M'Kacher et al., 2010; Bakhoum et al., 2011; Levine and Holland, 2018; Ben-David and Amon, 2020). Cells have well-conserved mechanisms to ensure proper chromosome segregation (Tanaka and Hirota, 2009), whose dysregulation may be involved in tumorigenesis. Therefore, chromosome missegregation is becoming a critical hallmark of tumor biology.

In this study, we determined a chromosome segregation-related gene prognostic signature from The Cancer Genome

Atlas (TACG) LUAD cohort. The distinct chromosome segregation regulators (CSRs)-related clusters of LUAD-samples were established, and the overall survival (OS) and the immune environment estimation were assessed in the distinct clusters. This study indicates that the CSRs were correlated with the poor prognosis and the possible immunotherapy resistance in LUAD, which might lay a theoretical foundation for the individualized treatment of LUAD-patients.

## MATERIALS AND METHODS

### Data Acquisition

The gene expression matrix (HTSEQ-Counts, HTSEQ-FPKM) for LUAD was acquired from the Genomic Commons Data Portal GDC (<https://portal.gdc.cancer.gov/>) of The Cancer Genome Atlas (TCGA) database (Tomczak et al., 2015), which contains 510 samples of patients and 58 normal samples. Clinical survival data ( $n = 738$ ) and phenotype data ( $n = 877$ ) of TCGA-LUAD matched patients were acquired from TCGA database. Excluding patients without information of survival, a total of 497 patients were retained for the prognostic analysis. For the nomogram model construction, 115 patients without information of the clinical index were excluded, and a total of 382 patients were retained.

The external validation sets of the Cox model were constructed using GSE3141 ( $n = 111$ ) (Bild et al., 2006), GSE13213 ( $n = 117$ ) (Tomida et al., 2009), GSE31210 ( $n = 226$ ) (Yamauchi et al., 2012), GSE30219 ( $n = 278$ ) (Rousseaux et al., 2013), and GSE50081 ( $n = 181$ ) (Der et al., 2014) datasets from the Gene Expression Omnibus (GEO) database (Barrett et al., 2013). The data was acquired by the GEOquery R package (Zhou J. et al., 2021).

### The Cox and Nomogram Model Construction

The gene expression matrix of the 48 CSRs in the 497 LUAD samples was used for the univariate cox regression, LASSO regression, and multivariate cox regression analyses. The Survival R package was used to calculate the correlation between the expression of each gene and overall survival (OS), and genes with a  $p$ -value  $< 0.05$  were retained for the following LASSO regression analysis. Glmnet and the survival R package were used for the LASSO regression analysis to screen the significant variables in the univariate cox regression

analysis. In order to obtain more accurate independent prognostic factors (prognostic characteristic genes), multivariate cox regression analysis was used for the final screening. The risk score was calculated as the follows: risk score = (exp-gene1\*coef-gene1) + (exp-gene n\*coef-gene n). Patients were divided into high- and low-risk groups based on the median of risk score.

Time-dependent receiver operating characteristic (ROC) curves were used to assess survival predictions, and the Time ROC R package was used to calculate the area under the ROC curve (AUC) value to measure prognosis and predict accuracy. Survcomp R package was used for the C-index analysis. For the nomogram analysis, the phenotype data ( $n = 382$ ) was used and the clinical indexes, including age, gender, race, TNM staging, and stage, were brought into the nomogram analysis. The calibration and decision curve analysis (DCA) were performed to assess the predictive power of the nomogram model.

The correlation of the 48 CSRs with the risk score was determined by Spearman correlation analysis. The Wilcoxon rank-sum test was used for the significant statistics.

## Identification of CSRs Pattern in LUAD Patients

Unsupervised clustering analysis (Testa et al., 2021) was used to identify the distinct clusters of LUAD patients according to the expression of 48 CSRs. R “Consensus Cluster Plus” package (Wilkerson and Hayes, 2010) was used for the clustering analysis.

## DEGs Determination and the Functional Enrichment Analysis

The differentially expressed genes (DEGs) were calculated using HTSEQ-FPKM of TCGA-LUAD by the Deseq 2 R package (Love et al., 2014), and visualized by the Ggplot 2 R package. The threshold is folded change > 2 and  $P_{adjust} < 0.05$ .

Gene Ontology (GO) (Ashburner et al., 2000) and pathway Kyoto Encyclopedia of Genes and Genomes (KEGG) (Ogata et al., 1999) enrichment were performed by the ClusterProfiler R package (Yu et al., 2012), and visualized by the Ggplot 2 R package.

## Identification of Hub Genes

The protein-protein interaction network was constructed by STRING (<https://cn.string-db.org/>) (Szklarczyk et al., 2019), and visualized by Cytoscape (v3.7.2) (Shannon et al., 2003). The rank of each gene in the network was calculated by CytoHubba (Chin et al., 2014). The Top 50 hub genes were chosen for the following analysis.

## TME Estimate Analysis

Stromal score, Immune score, ESTIMATE score, and Tumor purity score were calculated based on mRNA expression matrix (Count,  $n = 497$ ) by an estimate R package (Yoshihara et al., 2013). Immunization checkpoint block (ICB) assessment was performed by calculating the tumor immune dysfunction and exclusion (TIDE) score. This is a

kind of computing algorithm based on gene expression profiles (<http://tide.dfci.harvard.edu>) (Fu et al., 2020). The difference between HLA family and immune checkpoint genes between the two clusters was performed based on the TPM of these genes.

The immune cell infiltration was calculated respectively by CIBERSORT algorithm (Newman et al., 2015) and xCell algorithm (Aran et al., 2017). The gene expression matrix data (FPKM,  $n = 497$ ) were uploaded to CIBERSORT, and the 22 types of immune cell infiltration matrix were obtained. The distribution of the immune cell infiltration in each sample was shown using Ggplot 2 R package. The 38 types of cells in xCell algorithm were obtained by immunedeconv R package (Sturm et al., 2020).

The correlation of the 48 CSRs with immunocyte fraction was determined by Spearman correlation analysis. The Wilcoxon rank-sum test was used for the significant statistics.

## Correlation Analysis Between CSRs and TMB

For each tumor sample, the total number of somatic mutations (except silent mutations) detected in the tumor is defined as the tumor mutation burden (TMB) (Merino et al., 2020), TMB score for each sample was calculated, and the difference between the two clusters was performed. The correlation of the 48 CSRs with the TMB score was determined by Spearman correlation analysis. The Wilcoxon rank-sum test was used for the significant statistics.

## The Chemotherapeutics Forecast

The 50 hub genes were used for the chemotherapeutics forecast, which was performed using the mode of action (moa) module of the connectivity map (CMap, <https://clue.io/command>) (Gao et al., 2019).

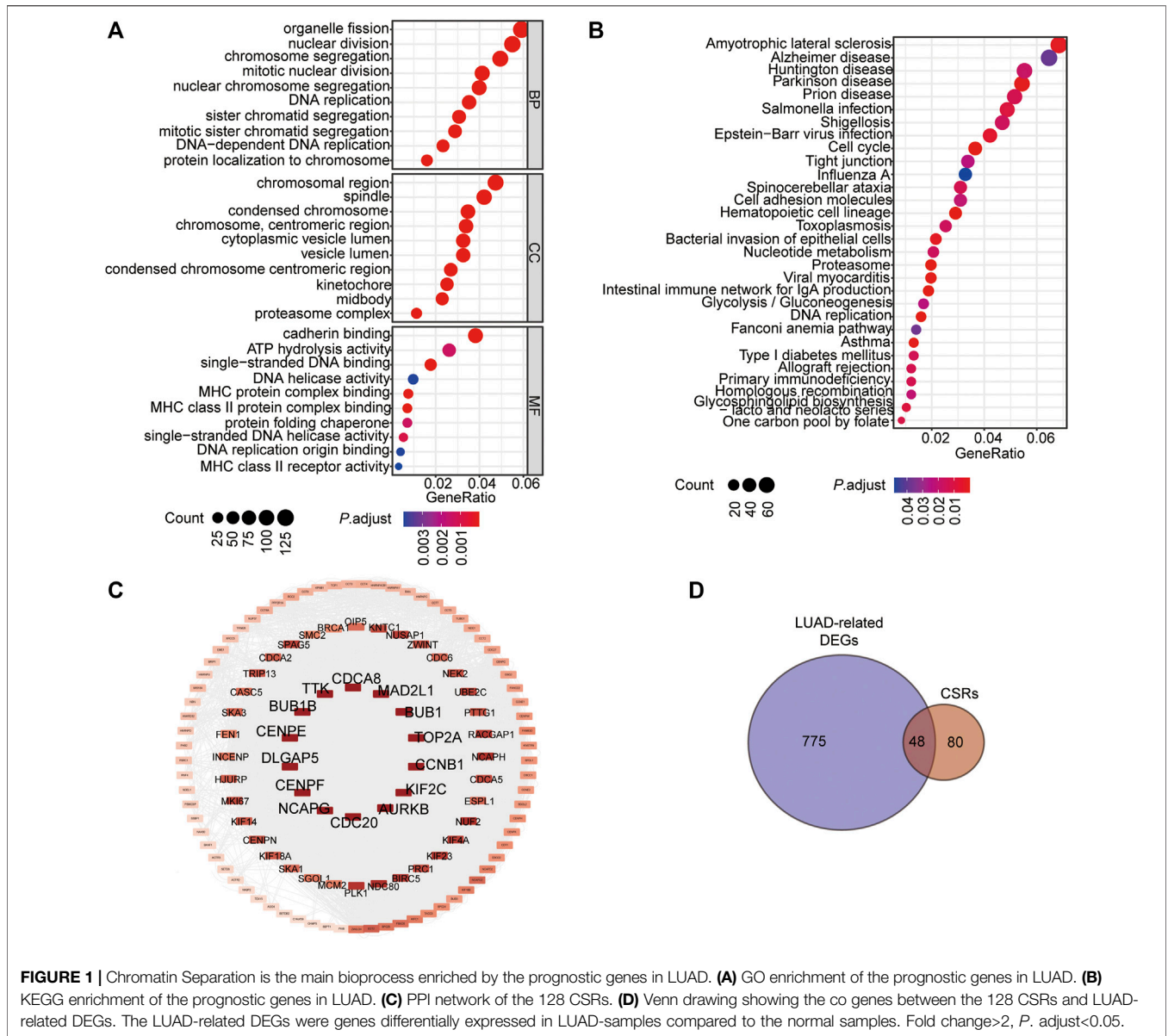
## Statistical Analysis

The statistical analysis was calculated via Wilcoxon rank-sum test and unpaired t-text. All statistical tests were bilateral. All statistical tests and visualization were performed in R software (version 4.0.2).

## RESULTS

### Chromatin Separation Is the Main Bioprocess Enriched by the Prognostic Genes in LUAD

To determine the significant genes involved in the prognosis of patients with LUAD, the batch prognostic analysis of whole genes in samples of TCGA-LUAD was performed. Among the 17,430 genes, a total of 2,416 genes significantly correlated with prognosis were obtained, with a threshold of  $p$ -value < 0.05 (**Supplementary Table S1**). GO and KEGG were performed to analyze the functional enrichment of these prognosis related genes, which showed that these genes were enriched in the biological processes of chromosome segregation, organelle



fission, and nuclear division, the cellular components of chromosomal region, condensed chromosome, centromeric region, spindle, and condensed chromosome, and molecular functions of cadherin binding, single-stranded DNA binding, and ATP hydrolysis activity (Figure 1A, Supplementary Table S2). Additionally, the KEGG pathways these prognostic genes were enriched in Amyotrophic Lateral sclerosis, Parkinson’s disease, Cell cycle, and DNA replication (Figure 1B, Supplementary Table S3). We noticed that chromosome segregation was the most significant bioprocess enriched by these genes (*P*.adjust = 5.5350E-19). We selected 128 genes enriched in the terms of chromosome segregation, nuclear chromosome segregation, and sister chromatid segregation for the subsequent analysis (Figure 1C, Supplementary Table S4), and we named them chromosome segregation regulators (CSRs). According to the calculated rank in the Protein-Protein

interaction (PPI) network (Figure 1C), the top 14 genes were selected, including centromere protein E (*CENPE*), mitotic arrest deficient 2 like 1 (*MAD2L1*), BUB1 mitotic checkpoint serine/threonine kinase (*BUB1*), BUB1 mitotic checkpoint serine/threonine kinase B (*BUB1B*), TTK protein kinase (*TTK*), cell division cycle 20 (*CDC20*), aurora kinase B (*AURKB*), aurora kinase B (*KIF2C*), DNA topoisomerase II alpha (*TOP2A*), DLG associated protein 5 (*DLGAP5*), non-SMC condensing I complex subunit G (*NCAPG*), cyclin B1 (*CCNB1*), centromere protein F (*CENPF*), and cell division cycle associated 8 (*CDCA8*) (Figure 1C, Supplementary Table S5). Among these genes, a total of 48 CSRs were found to overlap with the 823 DEGs in TCGA-LUAD (Figure 1D, Supplementary Table S6, Supplementary Table S7).

The Kaplan-Meier analysis showed that the 48 CSRs were all correlated with the poor OS in LUAD (Supplementary Figure

**TABLE 1** | Correlation of CSRs with Risk\_Score and TMB.

Gene Name	Risk_Score		TMB	
	Correlation (spearman)	p-Value	Correlation (spearman)	p-Value
AURKB	0.36	<2.2e-16	0.46	3.31e-27
BIRC5	0.41	<2.2e-16	0.43	2.04e-24
BUB1	0.45	<2.2e-16	0.45	5.99e-6
BUB1B	0.49	<2.2e-16	0.40	4.84e-21
CCNB1	0.48	<2.2e-16	0.38	2.92e-18
CCNE1	0.34	<4.4e-15	0.38	1.33e-18
CDC20	0.43	<2.2e-16	0.47	1.12e-28
CDC6	0.42	<2.2e-16	0.41	6.12e-22
CDCA2	0.46	<2.2e-16	0.38	8.74e-19
CDCA5	0.46	<2.2e-16	0.45	2.7e-26
CDCA8	0.41	<2.2e-16	0.45	8.53e-26
CDT1	0.38	<2.2e-16	0.37	6.67e-18
CENPE	0.45	<2.2e-16	0.39	7.37e-20
CENPF	0.43	<2.2e-16	0.40	6.8e-21
CENPK	0.36	<2.2e-16	0.30	1.53e-11
DLGAP5	0.5944	<2.2e-16	0.42	5.64e-23
EME1	0.26	2.8e-09	0.45	1.4e-26
ESPL1	0.3928	<2.2e-16	0.43	1.61e-23
FAM83D	0.43	<2.2e-16	0.36	2.19e-16
HJURP	0.5546	<2.2e-16	0.46	2.7e-28
KIF14	0.5192	<2.2e-16	0.43	8.08e-24
KIF18B	0.3933	<2.2e-16	0.43	2.17e-24
KIF23	0.5	<2.2e-16	0.44	5.55e-25
KIF2C	0.43	<2.2e-16	0.48	5.13e-30
KIF4A	0.45	<2.2e-16	0.40	4.16e-21
KIFC1	0.4	<2.2e-16	0.47	1.29e-28
KNTC1	0.21	3.2e-06	0.39	3.31e-19
MAD2L1	0.46	<2.2e-16	0.36	4.73e-17
MKI67	0.5	<2.2e-16	0.36	1.44e-16
NCAPG	0.46	<2.2e-16	0.43	1.49e-23
NCAPH	0.45	<2.2e-16	0.47	1.06e-28
NDC80	0.45	<2.2e-16	0.46	6.56e-26
NEK2	0.45	<2.2e-16	0.47	4.71e-29
NUF2	0.354	<2.2e-16	0.52	1.2e-34
NUSAP1	0.47	<2.2e-16	0.39	1.12e-19
OIP5	0.5075	<2.2e-16	0.40	5.67e-21
PLK1	0.6434	<2.2e-16	0.42	1.35e-22
PRC1	0.51	<2.2e-16	0.40	1.43e-20
SKA1	0.45	<2.2e-16	0.44	2.32e-25
SKA3	0.48	<2.2e-16	0.45	8.21e-27
SPAG5	0.38	<2.2e-16	0.46	9.98e-28
SPC24	0.35	2.3e-15	0.39	2.58e-19
SPC25	0.45	<2.2e-16	0.40	6.9e-21
TOP2A	0.38	<2.2e-16	0.45	6.78e-25
TRIP13	0.37	<2.2e-16	0.45	5.54e-27
TTK	0.41	<2.2e-16	0.47	1.48e-29
UBE2C	0.34	2.9e-15	0.47	1.04e-28
ZWINT	0.39	<2.2e-16	0.39	2.54-19

**S1**). In addition, the Spearman correlation analysis showed that these CSRs were positively associated with the high TMB in LUAD (**Table 1**). These indicated that the 48 CSRs may play important roles in LUAD progression.

### The CSRs Are Involved in LUAD Process

The 48 CSRs we identified were used to perform the Univariate Cox regression analysis in TCGA-LUAD ( $n = 497$ ), and 47 genes were eligible for screening ( $p$ -value < 0.05, **Supplementary Table S8**). The 47 genes were then chosen to perform the LASSO regression, and 12 genes were

screened out to build a multivariate Cox regression analysis (**Figures 2A,B, Supplementary Table S9**). Finally, 9 genes, including *PLK1*, *TTK*, *DLG* associated protein 5 (*DLGAP5*), Holliday junction recognition protein (*HJURP*), kinesin family member 14 (*KIF14*), Opa interacting protein 5 (*OIP5*), extra spindle pole bodies like 1, separase (*ESPL1*), kinesin family member 18B (*KIF18B*), and *NUF2* component of *NDC80* kinetochore complex (*NUF2*), were identified to be independent prognostic signatures (**Figures 2C,D, Supplementary Table S10, Supplementary Table S11**). The 497 LUAD samples were divided into two subgroups with

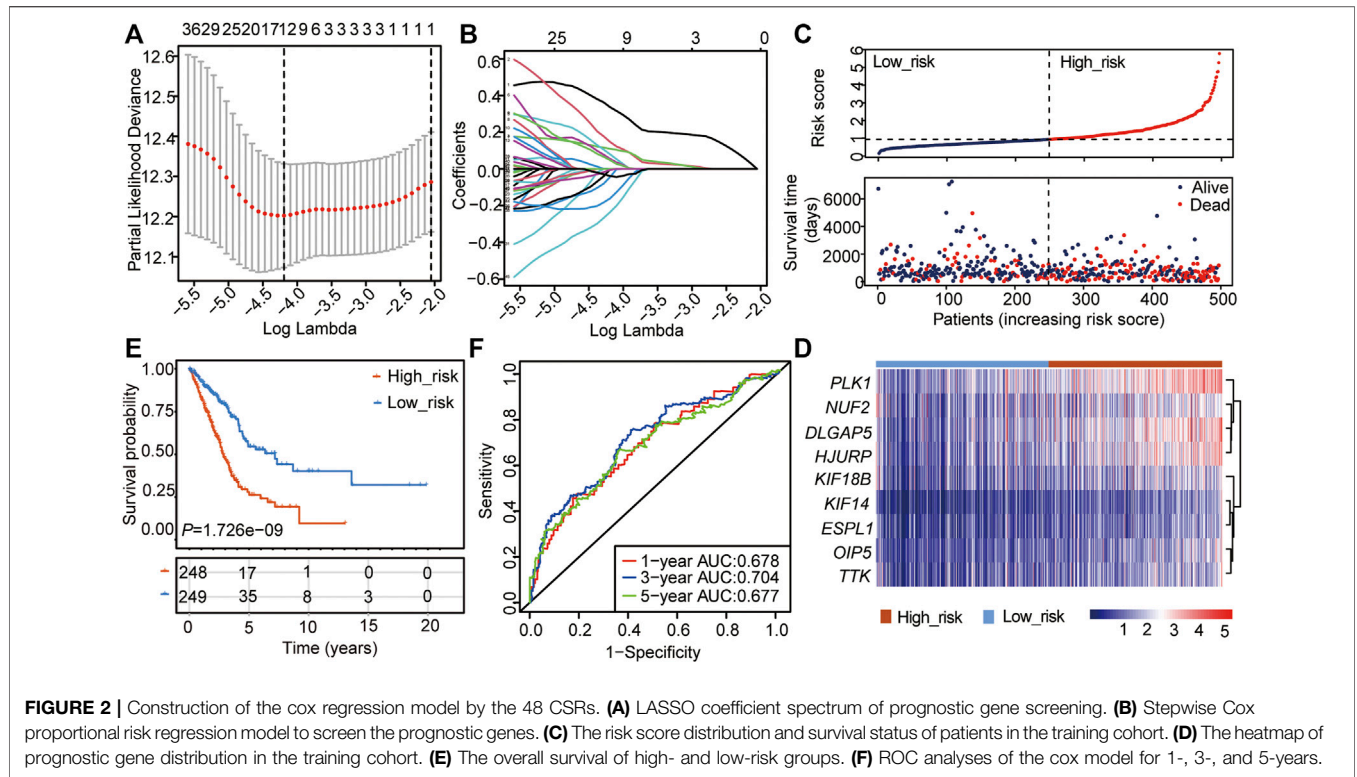


**TABLE 2 |** The clinical index of LUAD patients used in the Cox model.

Characteristic	Levels	Overall	High-Risk	Low-Risk
n (Dead/Alive)		382 (149/233)	204 (103/101)	178 (46/132)
Age, n (%)	>=65	213 (55.76%)	114 (53.52%)	98 (46.48%)
	<65	169 (44.24%)	90 (44.12%)	90 (55.88%)
Gender, n (%)	Male	170 (44.50%)	78 (45.88%)	92 (54.12%)
	Female	212 (55.50%)	126 (59.43%)	86 (40.57%)
N stage, n (%)	N0	249 (65.18%)	129 (51.80%)	120 (48.20%)
	N1	65 (17.01%)	40 (61.53%)	25 (38.47%)
	N2	56 (14.65%)	27 (48.21%)	29 (51.79%)
	N3	1 (0.26%)	1 (100%)	0 (0)
	NX	11 (2.90%)	7 (63.63%)	4 (36.37%)
M stage, n (%)	M0	241 (63.08%)	124 (51.45%)	117 (48.55%)
	M1	21 (5.49%)	8 (38.09%)	13 (61.91%)
	MX	120 (31.43%)	72 (60.00%)	48 (40.00%)
T stage, n (%)	T1	132 (34.55%)	75 (56.82%)	57 (44.18%)
	T2	196 (51.30%)	97 (49.49%)	99 (50.51%)
	T3	40 (10.47%)	22 (55.00%)	18 (45.00%)
	T4	13 (3.40%)	9 (69.23%)	4 (30.77%)
	TX	1 (0.28%)	1 (100%)	0 (0%)
Pathologic stage, n (%)	Stage I	209 (54.71%)	107 (51.20%)	102 (48.80%)
	Stage II	87 (22.77%)	53 (60.92%)	34 (39.08%)
	Stage III	59 (15.44%)	33 (55.93%)	26 (44.07%)
	Stage IV	21 (5.49%)	8 (38.10%)	13 (61.90%)
	N/A	6 (1.59%)	3 (50.00%)	3 (50.00%)

different risk scores: high- and low-risk subgroups, according to the median risk score based on the 9-gene independent prognostic signature (Figure 2C). The mortality of the high-risk group was higher than that of the low-risk group

(Figure 2C), and the patients in the high group had a poor outcome compared with those in the low-risk group ( $p = 1.726e-09$ , Figure 2E). Meanwhile, the 48 CSRs were all positively associated with the risk score (Figure 2D;

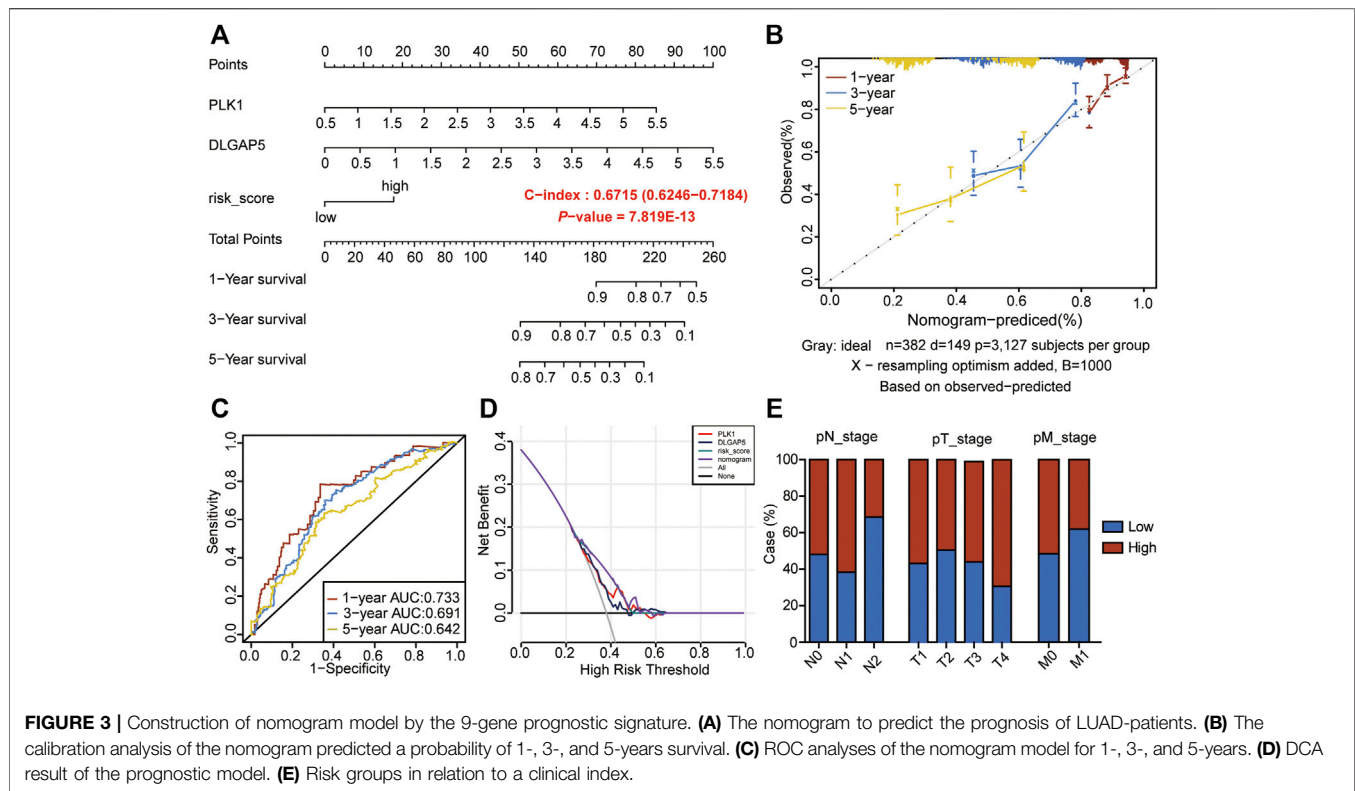


**TABLE 3 |** Information of GEO data sets used in the validation of the Cox.

Gene Name				
	GPL6480	117 (49/68)	58 (33/25)	59 (16/43)
GSE31210	GPL570	226 (35/191)	113 (28/85)	113 (7/106)
GSE30219	GPL570	278 (188/90)	139 (115/24)	139 (72/66)
GSE3141	GPL570	111 (58/53)	55 (33/22)	56 (25/31)
GSE50081	GPL570	181 (75/106)	91 (48/42)	90 (27/64)

**Table 1).** The ROC curve was used to predict the prognosis for 1-year, 3-years, and 5-years, which showed that the AUC value ranged from 0.628 to 0.73 (Figure 2F). These indicated that the high expression of CSRs predicts the poor OS in LUAD.

### Construction of Nomogram Model by the Nine-Gene Prognostic Signature

To further analyze the prognostic significance of the CSRs in LUAD patients, the 9-gene prognostic signature was used to perform the nomogram model with the combination of the clinical indexes, including pT\_stage, pN\_stage, pM\_stage, and stage (Table 2). Two significant genes (*PLK1* and *DLGAP5*) were brought into the nomogram model, which showed that the expression values of the two genes and the risk score predicted the survival of LUAD patients (Figures 3A,B). The ROC curve showed that the nomogram Cox model could precisely predict the survival of patients, with the AUC ranging from 0.642 to 0.733 (Figure 3C). The decision curve analysis (DCA) and calibration

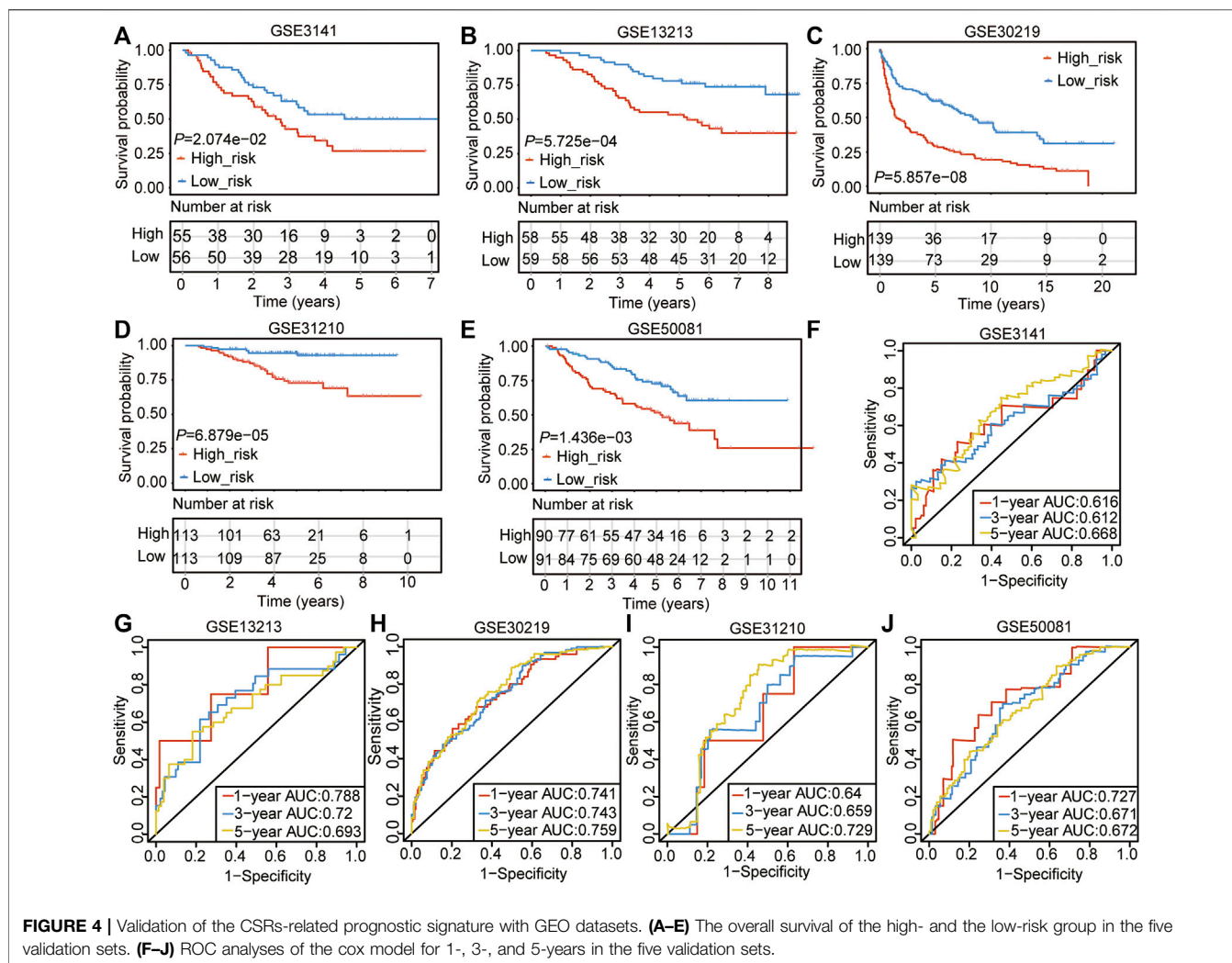
analysis of nomogram predicted probability also suggested the accuracy of the Cox model (Figures 3B,D). However, there was no significant difference in the pTNM staging between the two risk groups (Figure 3E).

### Validation of the CSRs-Related Prognostic Signature With GEO Datasets

We used the nine genes to conduct the Cox model in five GEO data sets (GSE3141, GSE13213, GSE30219, GSE31210, and GSE50081), which contains 913 LUAD samples (Table 3, Supplementary Table S12). The Kaplan-Meier curve showed the patients in the high-risk group had poor outcomes in the five validation sets (Figures 4A–E). The AUC value of 1-, 3-, and 5-years in the five validation sets were ranging from 0.612 to 0.788 (Figures 4F–J), which verified our previous results that the 9-gene prognostic signature was linked to predicting the OS of LUAD patients.

### Identification of Different Clusters Mediated by the 48 CSRs in LUAD.

To investigate the specific function of the CSRs involved in the development of LUAD, the unsupervised consensus clustering analysis was conducted for LUAD samples based on the expression of 48 CSRs. The result showed that the 497 LUAD samples were divided into two distinct subgroups of cluster 1 (C1,  $n = 338$ ) and cluster 2 (C2,  $n = 159$ ) (Figures 5A–D, Supplementary Table S13). The Kaplan-Meier curve showed



that patients in C1 had a worse outcome than those in C2 ( $p = 0.000351$ , **Figure 5E**). The difference in TMB score between the two clusters was assessed, and the result showed that C1 had a higher TMB score (**Figure 5F**). Moreover, the 48 CSRs were consistently highly expressed in group C1 compared with those in cluster 2 (**Figures 5G,H**, **Supplementary Table 14**), validating the existence of distinguishing CSRs patterns in LUAD, and the cluster 1 may represent high-risk groups.

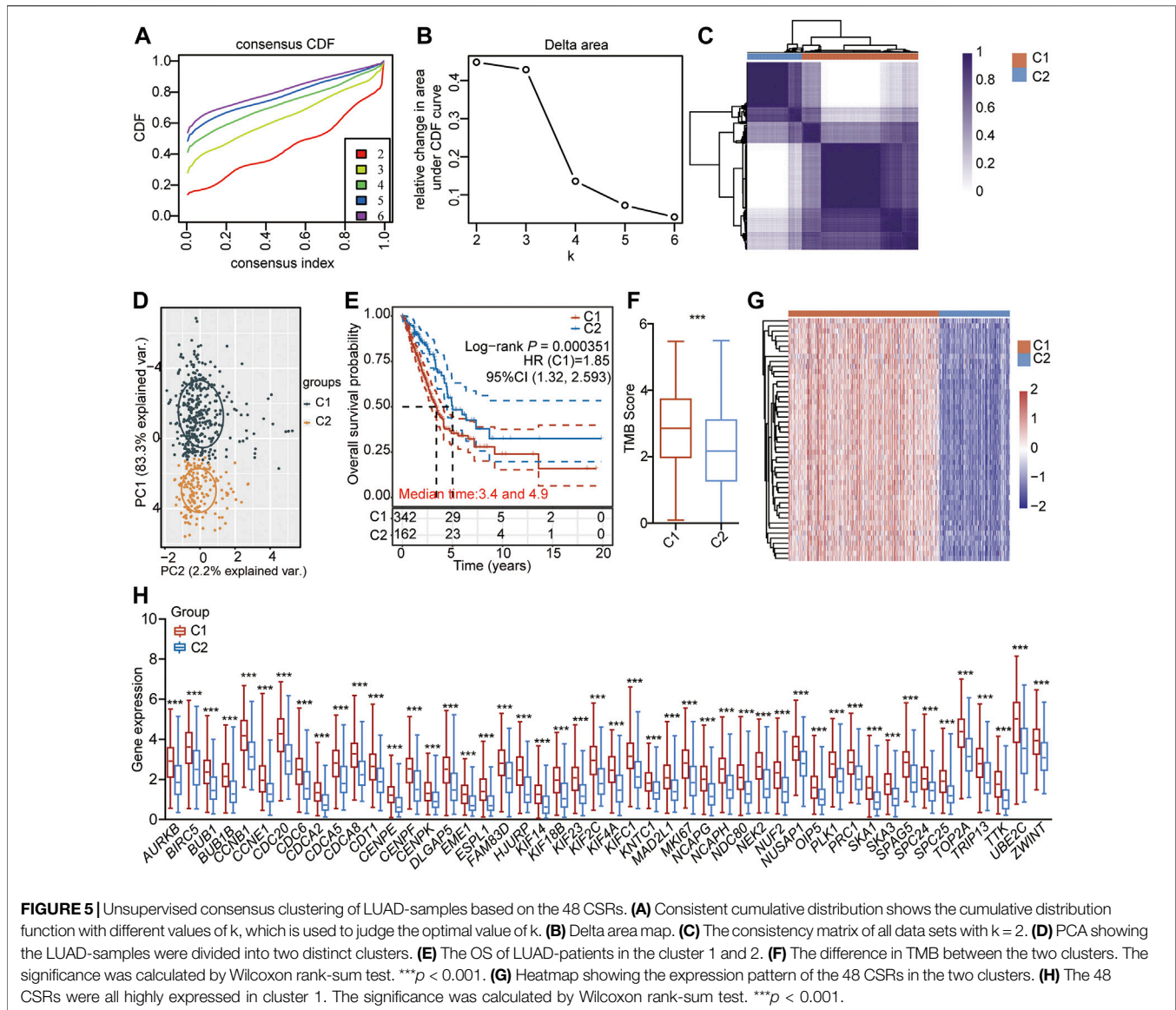
## DEGs and the Functional Analysis Between the Two CSRs-Related Clusters

Then, we identified the DEGs between the two clusters. As a result, a total of 536 genes (278 up-regulated genes and 258 down-regulated genes) were found to be significantly and differently expressed in group C1 compared to group C2 (**Figures 6A,B**, **Supplementary Table S15**). The subsequent KEGG and GO showed that the up-regulated genes were enriched in the pathways of cell cycle (**Figure 6C**, **Supplementary Table S16**), and the biological processes of chromosome segregation, organelle fission, and nuclear division, and mitotic nuclear division (**Figure 6D**,

**Supplementary Table S16**). The down-regulated genes were enriched in the pathways of Complement and coagulation cascades, Arachidonic acid metabolism, and Drug metabolism–cytochrome P450 (**Figure 6E**, **Supplementary Table S16**), and biological processes of antibacterial humoral response, eicosanoid biosynthetic process, protein processing, respond to corticosteroid, respond to glucocorticoid, and eicosanoid metabolic process (**Figure 6F**, **Supplementary Table S16**).

## Identification of Hub-Genes Between the Distinct Clusters

The 536 DEGs between the two CSRs-related clusters were used to perform the PPI network, which showed that there was an obvious group with a close correlation occurring in the up-regulated genes (**Figure 7A**). We calculated the rank by cytohubba in the PPI network, and the top 50 hub-genes were selected, which were all up-regulated genes in cluster 1 (**Figure 7B**, **Supplementary Table S17**). The subsequent GO showed these genes were enriched in the biological processes of the mitotic cell cycle, cell division, and regulation of chromosome segregation (**Figure 7C**).



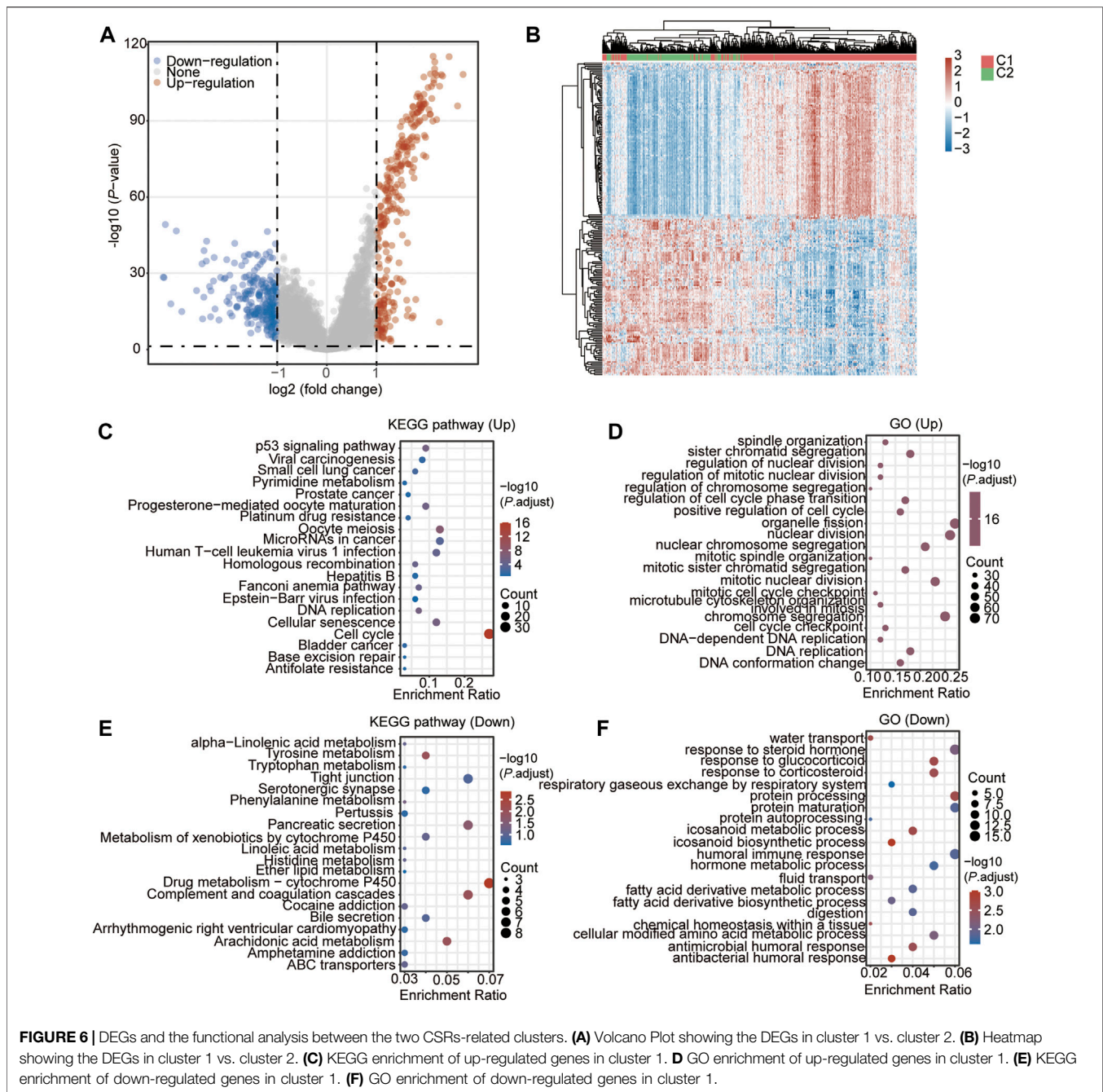
## CSRs Are Associated With Immunization Checkpoint Block in LUAD

Cancer cells must have evaded the anti-tumor immune response to grow progressively, which relies in part on the expression on their surface of proteins with immunosuppressive functions, such as programmed cell death 1 (PD-L1) (Reisländer et al., 2020). Enhanced ability to escape immune detection always caused malignant development of cancer cells, and the following poor outcome for patients with LUAD. To find out the possible molecular mechanism that the CSRs impact on the prognosis, the difference in immunization checkpoint block (ICB) score between the two clusters, including the levels of immune checkpoint genes, tumor immune dysfunction and exclusion (TIDE) score, and HLA component expression, were evaluated. We found that the C1 had a higher level of risk score ( $p = 2.26e-21$ , **Figure 8A**), and TIDE score ( $p = 1.8e-11$ ,

**Figure 8B**). Additionally, the immune checkpoint genes, CD274 (PD-L1), lymphocyte activating 3 (LAG3), programmed cell death 1 (PDCD1 (PD-1)), and programmed cell death 1 ligand 2 (PDCD1LG2), were significantly expressed higher in C1 than in C2 (**Figure 8C**). Moreover, among the eight MHC-II components, seven molecules were expressed lower in C1 than in C2 (**Figure 8D**). One MHC-I component was also expressed lower in C1 (**Figure 8D**). These all indicated that the patients in cluster 1 may have a higher immunization checkpoint block (ICB).

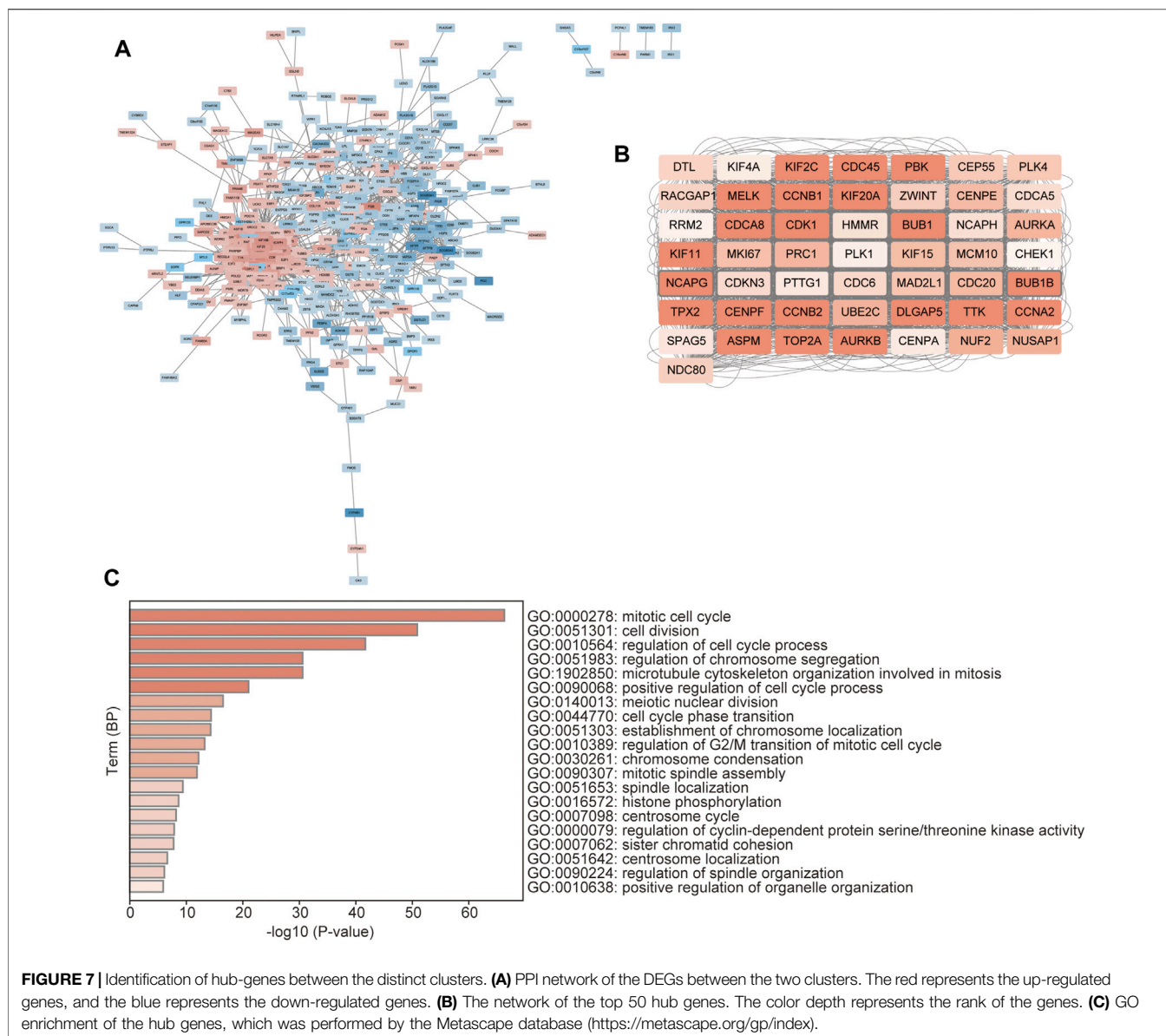
## CSRs Are Associated With Immune Characteristics of LUAD

To further explain the possible impact of the CSRs on anti-tumor immune response, the TME characteristics between the two clusters were also assessed. The result of TME showed that the



ESTIMATE score ( $p = 0.0042$ ), immune score ( $p = 0.0196$ ), and stromal score ( $p = 0.0017$ ) were lower in cluster 1 than in cluster 2 (Figures 9A–C), while the tumor purity ( $p = 0.003$ ) was higher in C1 than in C2 (Figure 9D). CIBERSORT algorithm was firstly used to calculate the 22 types of immune cells. The result showed that the filtrating proportion of resting memory CD4<sup>+</sup> T cells, activated mast cells, resting myeloid dendritic cells, and memory B cells were higher in cluster 2 than in cluster 1 (Figure 9E), while the filtrating proportion of follicular helper T cells, CD8<sup>+</sup> T cells, M0 macrophages, and M1 macrophages were higher in cluster 1 than in cluster 2 (Figure 9E). The xCELL algorithm was further

used to assess another immune cell set, which contains 35 kinds of immune cells. The result showed that the proportion of T cell CD8<sup>+</sup> naïve, Common lymphoid progenitor, CD4<sup>+</sup> Th2, CD4<sup>+</sup> Th1, plasmacytoid dendritic cell, and M1 macrophage were higher in cluster 1 (Figure 9F), while the content of activated myeloid dendritic cell, granulocyte-monocyte progenitor, mast cell, myeloid dendritic cell, M2 macrophage, memory CD4<sup>+</sup> effector T cells, and NK T cells were higher in cluster 2 (Figure 9F). Besides this, immune score, microenvironment score, and stroma score were lower in cluster 1 than in cluster 2, which was consistent with our previous result (Figure 9F).

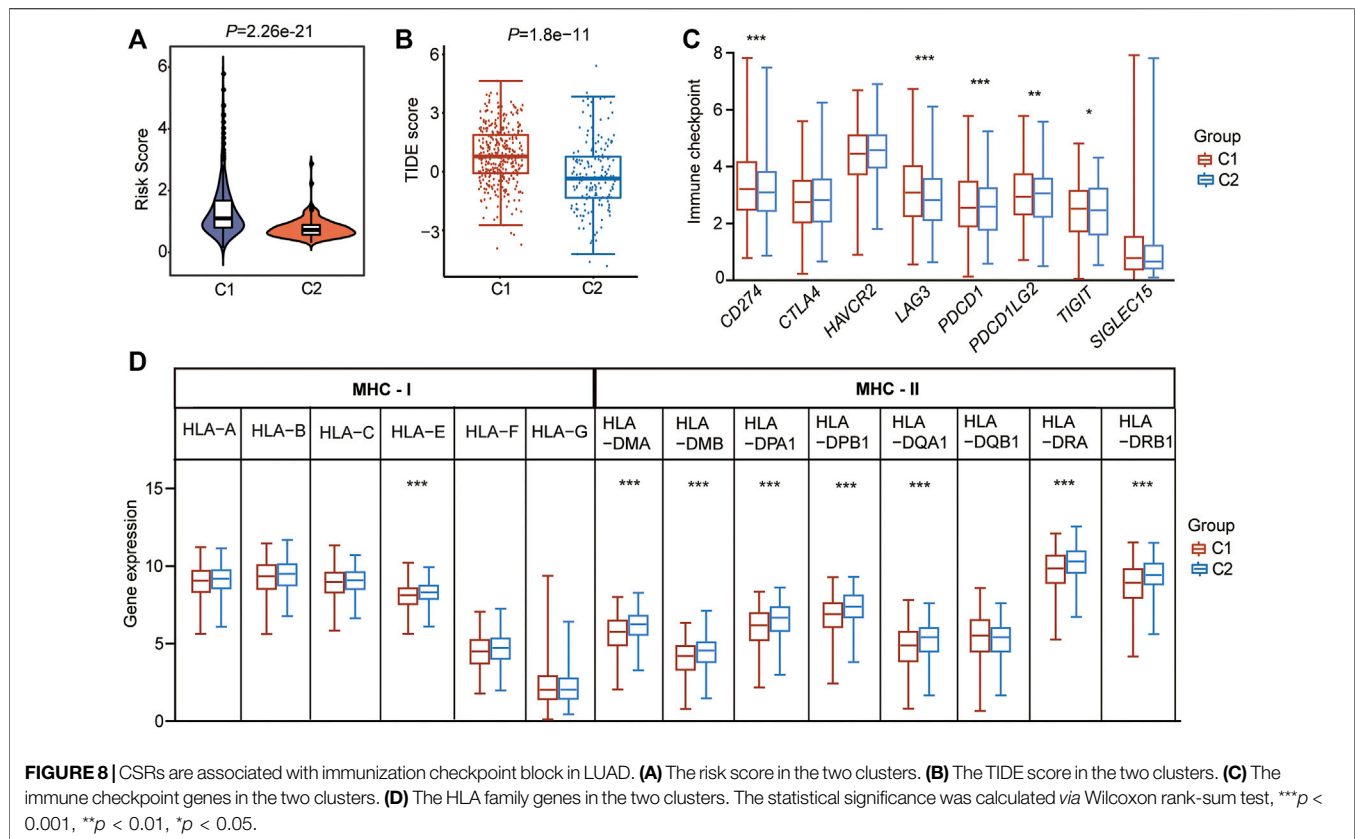


The difference in the abundance of 22 immune microenvironment infiltrating cells calculated by CIBERSORT algorithm between high- and low-risk groups in TCGA cohort and two GEO datasets was further revealed. The result in TCGA cohort showed that the high-risk group has a very similar pattern of infiltrated immune cells as the C1 population (Figure 9G). In addition, the infiltrating abundance of M0 and M1 macrophages were significantly higher in the high-risk group in all three datasets (Figure 9G, Supplementary Figure S2), and the filtering proportion of resting memory CD4<sup>+</sup> T cells was lower in the high-risk group compared to the low-risk group in all three datasets (Figure 9G, Supplementary Figure S2), indicating that the nine-gene independent prognostic signature was positively correlated with the infiltrating abundance of M0 and M1 macrophages and negatively associated with resting memory CD4<sup>+</sup> T cells. These all demonstrated that the CSRs

were associated with the immune characteristics in the TME of LUAD.

## The Small-Molecular Chemotherapeutics Forecast for High-Risk Patients Based on the Hub-Genes

Our previous results showed that patients in cluster 1 were the predicted high-risk population, and we then wanted to find the potential chemotherapeutics suited for these populations. According to the different biological characteristics between the two clusters, the hub genes were assumed to be the critical and potential targets for the therapy of the high-risk groups. Therefore, the adjuvant chemotherapeutics targeting the 50 hub genes were assessed through the mode of action (moa) module in the CMap database. The result showed that a total of 74 small-



molecular perturbagens, targeting aurora kinase B (*AURKA*), cyclin-dependent kinase 1 (*CDK1*), *TOP2A*, *AURKB*, polo-like kinase 4 (*PLK4*), *PLK1*, ribonucleotide reductase regulatory subunit M2 (*RRM2*), *CCNB1*, *TTK*, and cyclin A2 (*CCNA2*), were predicted to be the potential chemotherapeutics for patients in cluster 1 (Figure 10). A total of 47 moas were predicted to be the possible pathways by which these chemotherapeutics function, such as Aurora kinase inhibitor, CDK inhibitor, and topoisomerase inhibitor (Figure 10). Among the 74 potential chemotherapeutics, AT-9283, indirubin, and LY-294002 were the most outstanding ones, which function as the most common pathways (marked in blue, Figure 10).

## DISCUSSION

Lung cancer is the most common malignancy and remains the leading cause of cancer mortality worldwide (Bade and Cruz, 2020). Approximately 85% of patients have a histological subtype known as non-small cell lung cancer (NSCLC) (Herbst et al., 2018), with the main subtype of LUAD (Herbst et al., 2018; Sun and Zhao, 2019). Recently, LUAD has been the major cause of cancer-associated mortality with a poor prognosis (Song et al., 2021). Chromosomal abnormalities are reported to be a common characteristic of cancer, which is attributed to the ongoing chromosome segregation errors during mitosis (Bakhom et al., 2018; Kou et al., 2020a). It is associated with poor outcomes and therapeutic resistance in various cancers

(Potapova and Gorbsky, 2017; Bakhom and Cantley, 2018; Kou et al., 2020a). Chromosomal segregation errors or the alteration of CSRs are usually the critical factors of genomic instability that drive tumor evolution (Hanahan and Weinberg, 2011; Bolhaqueiro et al., 2019; Tayoun et al., 2021). For example, aneuploidy is a direct consequence of chromosome segregation errors in mitosis (Janssen et al., 2011; Kawakami et al., 2019). This is always accompanied by chromosomal instability (CIN) and genomic instability and causes additional chromosome gains or losses in a significant proportion of cell divisions, which further manifests the complexity of cancer karyotypes (Dürbaum and Storchová, 2016). Aneuploidy correlates with increased metastatic and drug resistance, indicating that Aneuploidy is more beneficial for cancerous cells than diploid cells (Dürbaum and Storchová, 2016). The genomic diversification caused by chromosome segregation errors usually promotes tumor evolution and heterogeneity (Soto et al., 2019), which is an important reason for therapeutic resistance (Dagogo-Jack and Shaw, 2018; Lim and Ma, 2019). Although aneuploidy provides advantages for the proliferation and drug resistance of cancer cells, excessive aneuploidy beyond a critical level is lethal to cancer cells (Kawakami et al., 2019). Therefore, molecular and bioprocesses engaged in chromosome segregation should be utilized as potential therapeutic targets for cancers.

Previous studies have indicated that CIN and loss of heterozygosity (LOH) play significant roles in the development of LUAD (Ninomiya et al., 2006). In this study, chromosomal segregation during mitosis was found to be correlated with the

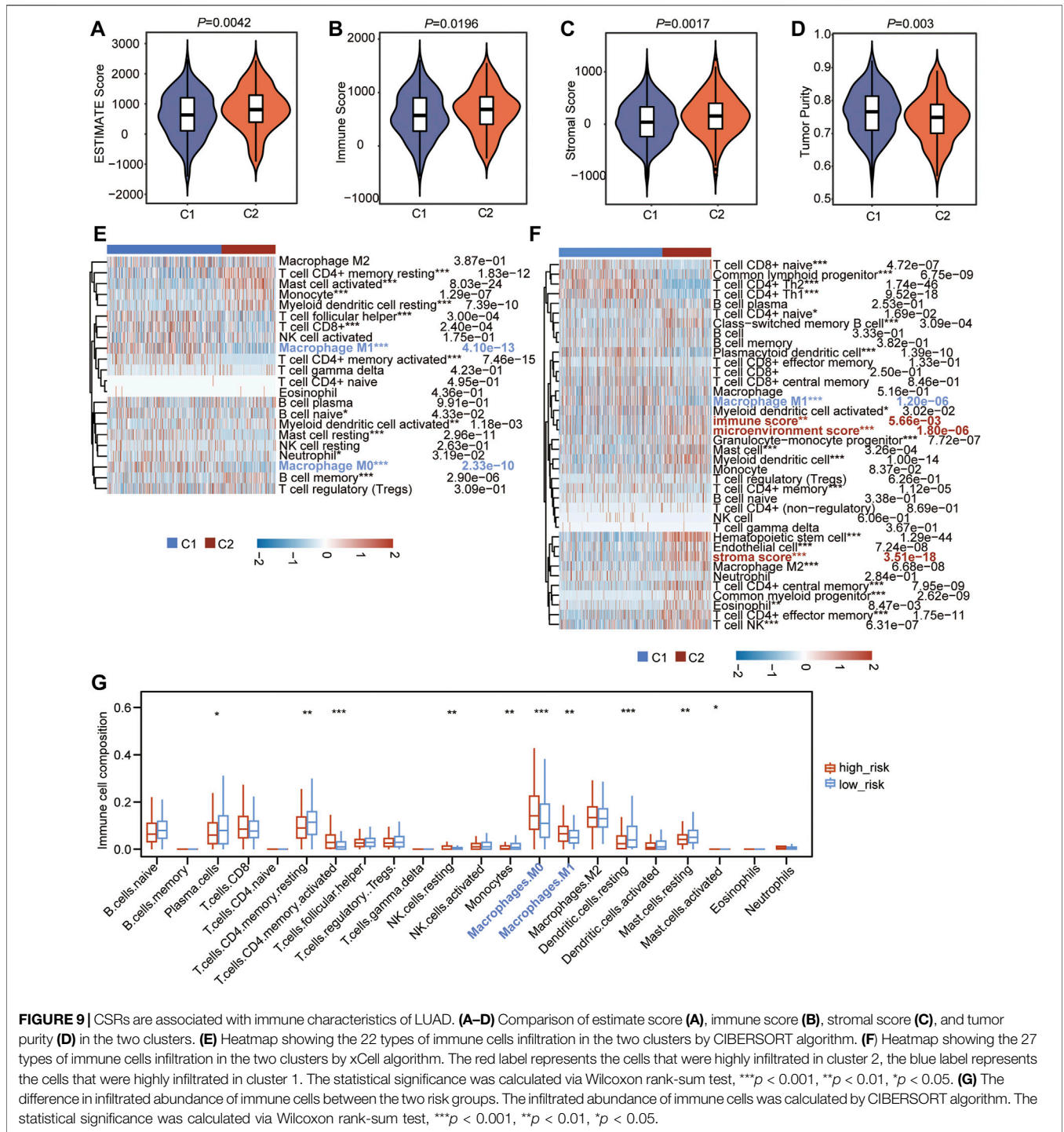
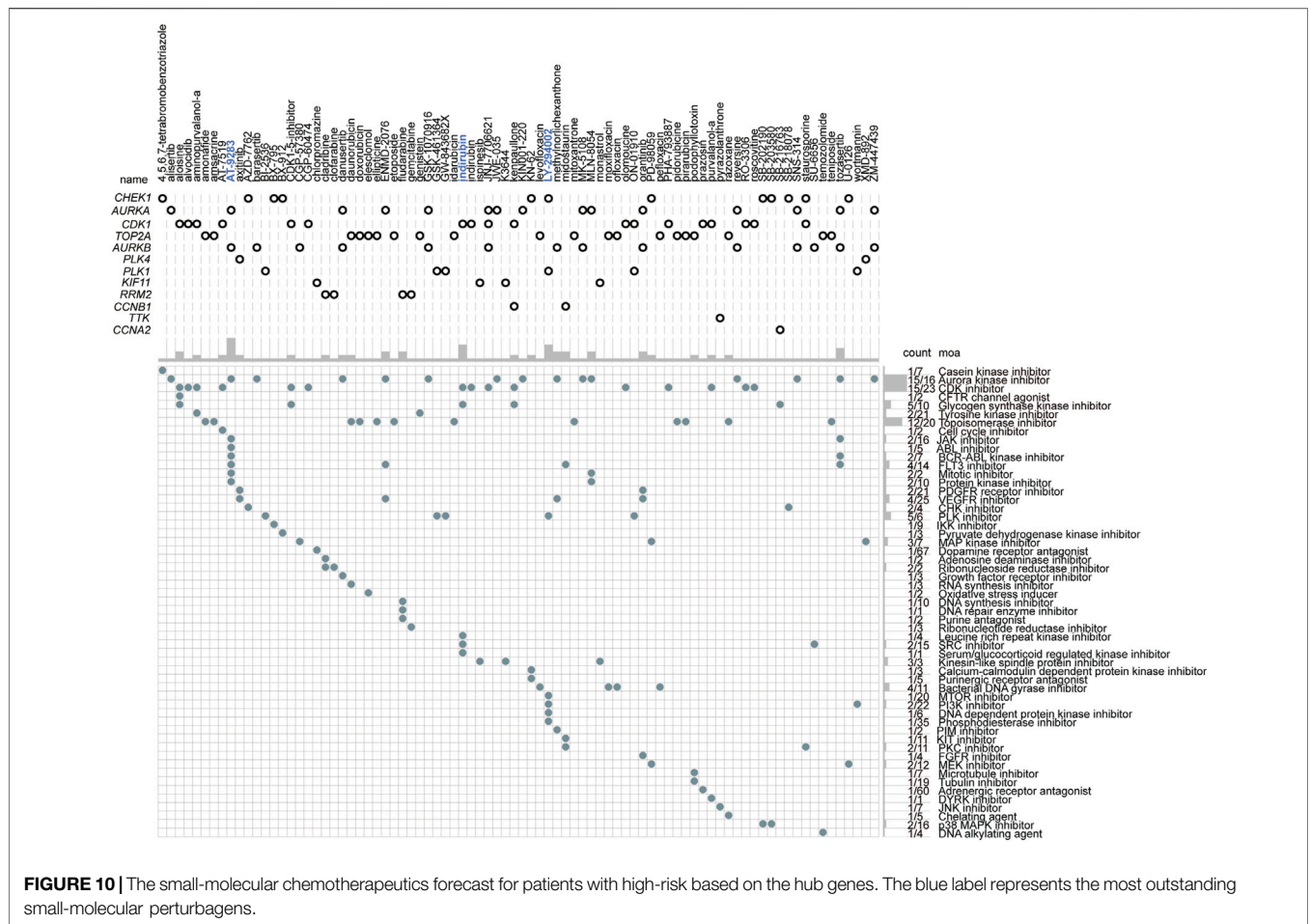


**FIGURE 9 |** CSRs are associated with immune characteristics of LUAD. **(A–D)** Comparison of estimate score **(A)**, immune score **(B)**, stromal score **(C)**, and tumor purity **(D)** in the two clusters. **(E)** Heatmap showing the 22 types of immune cells infiltration in the two clusters by CIBERSORT algorithm. **(F)** Heatmap showing the 27 types of immune cells infiltration in the two clusters by xCell algorithm. The red label represents the cells that were highly infiltrated in cluster 2, the blue label represents the cells that were highly infiltrated in cluster 1. The statistical significance was calculated via Wilcoxon rank-sum test, \*\*\* $p < 0.001$ , \*\* $p < 0.01$ , \* $p < 0.05$ . **(G)** The difference in infiltrated abundance of immune cells between the two risk groups. The infiltrated abundance of immune cells was calculated by CIBERSORT algorithm. The statistical significance was calculated via Wilcoxon rank-sum test, \*\*\* $p < 0.001$ , \*\* $p < 0.01$ , \* $p < 0.05$ .

poor prognosis of LUAD. Among the determined 2,416 prognosis-related genes, 128 genes were found to be enriched in the biological processes of chromosomal segregation, indicating that these chromosomal segregation-related genes may play an important role in the development of LUAD. 48 of 128 genes were found to be up-regulated in LUAD compared with the normal people and were associated with the high TMB in patients with LUAD. Besides, 47 genes were

identified as the prognostic signatures after suffering from univariate cox regression. By LASSO and multivariate cox regression, nine genes were finally determined as the independent prognostic signature to construct the nomogram cox model. Patients in the high-risk subgroup had significantly poor OS. Notably, *PLK1* and *DLGAP5* were found to have valuable significance for the prediction of prognosis. *PLK1* plays multiple roles in the initiation, maintenance, and



completion of mitosis (Liu et al., 2017), maintaining genome stability (Zhang et al., 2016; Gheghiani et al., 2021), and DNA damage response (DDR) (Peng et al., 2021). It is found to be highly expressed in most of the human cancers (Gutteridge et al., 2016), and enhanced gene expression is associated with a poor prognosis (Ramani et al., 2015; Tut et al., 2015; Zhang et al., 2015; Chen Z. et al., 2019; Montaudon et al., 2020). Besides, PLK1 has been reported to be associated with chemotherapeutic drugs resistance, including doxorubicin (Wang P. et al., 2018), paclitaxel (Gasca et al., 2016; Shin et al., 2019; Shin et al., 2020), metformin (Shao et al., 2015; Zhu et al., 2022), and gemcitabine (Song et al., 2013; Li et al., 2016; Mao et al., 2018). DLGAP5 is a microtubule-associated protein and is identified to be a prognosis biomarker in various cancers (Schneider et al., 2017; Branchi et al., 2019; Xu et al., 2020; Zheng et al., 2020; Feng Y. et al., 2021; Zhou D. et al., 2021). Inhibition of this gene suppresses cell proliferation and invasion, induces G<sub>2</sub>/M phase arrest, and promotes apoptosis in human cancers (Liao et al., 2013; Zhang et al., 2021a). Not only these findings were confirmed, but also the predictive value of the two genes was proposed in this study. Here, *PLK1* and *DLGAP5* were found as the independent prognostic signatures combined with *HJURP*, *KIF14*, *OIP5*, *TTK*, *ESPL1*, *KIF18B*, and *NUF2* to predict the prognosis of LUAD-patients. *HJURP* is reported to be an

oncogene that promotes cancer cell proliferation, migration, and invasion (Chen et al., 2018; Wei et al., 2019; Serafim et al., 2020; Li Y. et al., 2021; Lai et al., 2021). *KIF14* is confirmed to promote cancer cell proliferation and contribute to chemoresistance (Singel et al., 2014; Wang Z. Z. et al., 2018; Xiao et al., 2021). Silencing *TTK* is also found to inhibit the proliferation and invasion and increase radiosensitivity and chemosensitivity of cancer cells (Chen S. et al., 2019; Huang et al., 2020; Liu Y. et al., 2021; Zhang et al., 2021b; Qi et al., 2021). *ESPL1* is determined to be a novel prognostic biomarker and is associated with the malignant features in several cancers (Finetti et al., 2014; Wang R. et al., 2020; Liu Z. et al., 2021). *KIF18B* is also illustrated to be the oncogenesis to promote tumor progression and enhance therapeutic resistance (Li B. et al., 2020; Liu et al., 2020; Jiang J. et al., 2021). *OIP5* upregulation is observed in human cancers (Chow et al., 2021), and seems to be linked to drug resistance (Rodrigues-Junior et al., 2018). *NUF2* is found to be a prognostic biomarker and therapeutic target which is correlated with the immune infiltration in patients with cancer (Jiang X. et al., 2021; Shan et al., 2021; Xie et al., 2021). Combining the expression of the nine genes, we conducted the cox risk model. The subsequent DCA and calibration verified the accuracy of the model to predict the prognosis of LUAD. However, we found the nine-gene prognostic signature had no impact on the

clinical pNTM stage of patients. This may be attributed to the small sample size, thus, larger samples should be analyzed further.

According to the unsupervised consensus clustering by the expression of the 48 CSRs, the 497 TCGA-LUAD samples were divided into clusters 1 and 2. The 48 CSRs were all highly expressed in cluster 1, and the risk score was significantly higher in cluster 1. The Kaplan-Meier showed that patients in cluster 1 had a poor OS. These all suggest that the patients in cluster 1 have a higher risk than those in cluster 2, and the subgroup cluster 1 is deemed to be the high-risk group. A total of 536 genes (278 up-regulated genes and 258 down-regulated genes) were determined to be the DEGs in cluster 1 compared to cluster 2. The up-regulated genes were enriched in the pathways of cell cycle and the biological processes of chromosome segregation, organelle fission, and nuclear division; the down-regulated genes were enriched in the pathways of drug metabolism-cytochrome P450 and the biological process of protein processing. The main function of cytochrome P450 (CYP450) is oxidative catalysis of endogenous and exogenous substances (Mittal et al., 2015). 80% of drugs currently in use, including anti-cancer drugs, are involved in phase I metabolism of CYP450 (Mittal et al., 2015). Interestingly, the hub genes with top 50 ranks were all highly expressed in cluster 1, which were enriched in the biological processes of mitotic cell cycle, regulation of chromosome segregation, and microtubule cytoskeleton organization involved in mitosis. As we discussed previously, the dysregulation of mitotic chromosome segregation is associated with poor prognosis and therapeutic resistance in human cancers. Among the 50 hub genes, *AURKB*, *BUB1*, *BUB1B*, *CCNB1*, *CDCA8*, *CENPF*, *DLGAP5*, *KIF2C*, *NCAPG*, *TOP2A*, *TTK*, assembly factor for spindle microtubules (*ASPM*), cyclin A2 (*CCNA2*), cyclin B2 (*CCNB2*), cell division cycle 45 (*CDC45*), cyclin-dependent kinase 1 (*CDK1*), kinesin family member 11 (*KIF11*), kinesin family member 20A (*KIF20A*), maternal embryonic leucine zipper kinase (*MELK*), PDZ binding kinase (*PBK*), TPX2 microtubule nucleation factor (*TPX2*) were found to be the hub genes with the rank 1, that were all reported to have prometastatic effects in human cancers (Chen et al., 2015; Bertran-Alamillo et al., 2019; Gan et al., 2019; Huang et al., 2019; Kou et al., 2020b; Wang L. et al., 2020; Wang X. et al., 2020; Hu et al., 2021; Wang S. et al., 2021; Li M.-X. et al., 2021; Wu et al., 2021; Feng Z. et al., 2021; Huang et al., 2021).

The difference in ICB between the two clusters was further assessed, including TIDE score, immune checkpoint genes, HLA family components to evaluate the possible anti-tumor immune response associated with the CSRs. The cluster 1 subtype featured lower levels of HLA family genes, higher TIDE scores, and higher levels of immune checkpoint genes, indicating that patients in cluster 1 have the higher ICB and, in turn, a possible poor anti-tumor immune response. The highly expressed immune checkpoint genes, *CD274*, *LAG3*, *PDCD1*, *PDCD1LG2*, in this subgroup further confirmed the result. *PDCD1* (PD-1) is a key coinhibitory receptor expressed on activated T cells (Ai et al., 2020). The engagement with its ligands, mainly PD-L1, leads to the events of inhibition of T cell proliferation, activation, cytokine production, alters metabolism and cytotoxic T lymphocytes

(CTLs) killer functions, and eventual death of activated T cells (Ai et al., 2020). The overexpression of PD-L1 has been verified to contribute to the immune surveillance evasion of cancer cells and caused the invasion and migration (Iwai et al., 2002). *PDCD1LG2* (PD-L2) is a second ligand for PD-1 and inhibits T cell activation (Latchman et al., 2001). *LAG3* (CD223), an emerging targetable inhibitory immune checkpoint molecule, is the third inhibitory receptor pathway to be targeted in the clinic (Solinas et al., 2019). It is mainly found on activated immune cells and is involved in the exhaustion of T cells in malignant diseases (Puhr and Ilhan-Mutlu, 2019). *LAG3* has been reported to play a negative regulatory role in cancer immunology by interacting with its ligands (Wang M. et al., 2021). What's more, seven MHC-II and one MHC-I molecules were found to be under-expressed in cluster 1, further supporting the result that patients in cluster 1 have a poor antitumor immune response. MHC-I molecules function to bind the encoded peptides, transport and display the antigenic information on the cell surface, and allow CD8<sup>+</sup> T cells to identify pathological cells, such as cancers that are expressing mutated proteins (Dhatchinamoorthy et al., 2021). Loss of MHC-I antigen presentation always leads to cancer immune evasion (Dhatchinamoorthy et al., 2021). MHC-II is an antigen-presenting complex, that is important for antigen presentation to CD4<sup>+</sup> T cells. Tumor-specific MHC-II is associated with favorable outcomes in patients with cancer, including those with immunotherapies (Axelrod et al., 2019). The lower level of MHC-II and one MHC-I molecule in patients of cluster 1 may help the tumor evasion of immune checkpoints and poor immunotherapies. What's more, we found a higher TMB score in cluster 1, which was positively associated with the 48 CSRs. A recent study has shown that the average copy number variation (CNVA) of chromosome fragments is a potential surrogate for tumor mutational burden in predicting responses to immunotherapy in NSCLC (Lei et al., 2021). Therefore, the increased genomic instability in tumors with dysregulated chromosome segregation alters mutational load and in turn impacts antitumoral immune responses, which further impacts the prognosis in LUAD. However, we cannot define either CIN as a cause or result of somatic mutation, and this needs more experiment assays to be determined.

Meanwhile, the infiltrating proportions of immune cells were further evaluated to analyze the difference in immune characteristics between the two clusters. We found that cluster 1 had a lower immune, stromal, and ESTIMATE score compared with cluster 2. According to the CIBERSORT and xCell algorithms, cluster 1 was shown to have a higher infiltrating proportion of M0 and M1 macrophages, while cluster 2 had a higher infiltrating proportion of M2 macrophages and mast cells. Macrophages play a critical role in cancer development and metastasis, which could be identified as 2 major subpopulations of M1 macrophages (Proinflammatory) and M2 macrophages (anti-inflammatory) (Xia et al., 2020). M0 macrophages are naïve macrophages without polarization. M1 macrophages have antimicrobial and antitumoral activity, while M2 macrophages participate in angiogenesis, immunoregulation, tumor formation, and progression (Shapouri-Moghaddam et al., 2018). Increased mast cell density is associated with the prognosis and plays a multifaceted role in TME by regulating tumor biology, including cell proliferation, angiogenesis, invasiveness, and

metastasis (Aponte-López and Muñoz-Cruz, 2020). These results seem contradictory that M1 macrophages have antitumoral activity but were higher infiltrated in cluster 1, whereas M2 macrophages have protumoral activity but were lower infiltrated in cluster 1, as were the follicular helper T cells and CD8<sup>+</sup> T cells. We think this elevation may be a compensatory effect, that these antitumoral immune cells are regulated to increase against the tumor cells. However, the effective activity of these anti-tumor immune cells may be inhibited because of the high levels of the immunosuppressive proteins on their surface. Most tumor-infiltrating immune cells were functionally inactive.

Based on the 50 hub genes that were upregulated in cluster 1, a total of 74 small-molecule perturbagens were predicted to be the potential chemotherapeutics that were possibly suited for these patients at high risk. Among these, AT-9283, indirubin, and LY-294002 were the most outstanding ones, which function as the most common pathways. A total of 47 moas, including Aurora kinase inhibitor, CDK inhibitor, and topoisomerase inhibitor, were forecasted to be the possible molecular mechanism by these chemotherapeutics functions. The inhibitory role of AT-9283 in cancer cell growth and survival has been demonstrated in cell-based systems (Kimura, 2010). Although phase II clinical trials have not been completed, it showed good safety and efficacy in phase I clinical trials conducted in patients with hematological malignancies and solid tumors (Kimura, 2010). Indirubin has also been reported to exert anticancer effects in human cancers (Li Z. et al., 2020). LY-294002 enhances the chemosensitivity of liver cancer to oxaliplatin (Xu et al., 2021). We found here these small-molecule perturbagens might have favorable therapeutic effects for patients in cluster 1, who had the high expression of their target genes. This will provide an effective therapeutic regimen for the individual treatment in LUAD.

Our study is the first one to systematically analyze the relationship between chromosome segregation regulation and the immune microenvironment. This can provide a new direction for immune-related LUAD pathogenesis and therapeutic research. However, there are certain limitations in this current study. First, although the exploration of a decent number of samples and summarizing data can be helpful in the research community, this analysis may have some bias due to the small size of TCGA-LUAD cohort. The relationship between the prognostic signatures and clinical indices, such as pNTM staging, has not been well explained. Therefore, further analysis with larger samples is still needed. Second, further experimental verifications are necessary to elucidate the potential impact of these predicted genes in the immune microenvironment. Moreover, the protein expression levels of the hub CSRs in

pathogenesis and progression of LUAD depend on further experimental studies to elucidate. Additionally, some of the genes we focused on in this study have been reported to be activated by post-translational modification and function as kinase. Therefore, database analyses depending on the gene expression profile at the mRNA levels have a limit. Further analysis should be focused on the protein or post-translational modification levels.

In conclusion, this study demonstrated that the CSRs were important factors to influence the development and progression of LUAD. The high expression of these regulators was correlated with the poor prognosis and the possible immunotherapeutic resistance in LUAD, which could be the potential therapeutic target for LUAD.

## DATA AVAILABILITY STATEMENT

The datasets presented in this study can be found in online repositories. The names of the repository/repositories and accession number(s) can be found in the article/**Supplementary Material**.

## AUTHOR CONTRIBUTIONS

ZL, GZ, and XZ designed experiments and interpreted data. ZL, ZM, HX, RS, KQ, and YZ conducted bioinformatic and statistical analyses. ZL wrote the paper. All authors have read and approved the manuscript for publication. GZ conceived the concept, designed the manuscript, coordinated, and critically revised manuscript, and was responsible for its financial supports and the corresponding works.

## FUNDING

This work was supported by grants from the Natural Science Foundation of Shandong Province (ZR2021MH274 to XZ.).

## SUPPLEMENTARY MATERIAL

The Supplementary Material for this article can be found online at: <https://www.frontiersin.org/articles/10.3389/fgene.2022.917150/full#supplementary-material>

## REFERENCES

- Ai, L., Xu, A., and Xu, J. (2020). Roles of PD-1/pd-L1 Pathway: Signaling, Cancer, and beyond. *Adv. Exp. Med. Biol.* 1248, 33–59. doi:10.1007/978-981-15-3266-5\_3
- Aponte-López, A., and Muñoz-Cruz, S. (2020). Mast Cells in the Tumor Microenvironment. *Adv. Exp. Med. Biol.* 1273, 159–173. doi:10.1007/978-3-030-49270-0\_9
- Aran, D., Hu, Z., and Butte, A. J. (2017). xCell: Digitally Portraying the Tissue Cellular Heterogeneity Landscape. *Genome Biol.* 18 (1), 220. doi:10.1186/s13059-017-1349-1
- Ashburner, M., Ball, C. A., Blake, J. A., Botstein, D., Butler, H., Cherry, J. M., et al. (2000). Gene Ontology: Tool for the Unification of Biology. The Gene Ontology Consortium. *Nat. Genet.* 25 (1), 25–29. doi:10.1038/75556
- Axelrod, M. L., Cook, R. S., Johnson, D. B., and Balko, J. M. (2019). Biological Consequences of MHC-II Expression by Tumor Cells in Cancer. *Clin. Cancer Res.* 25 (8), 2392–2402. doi:10.1158/1078-0432.ccr-18-3200
- Bade, B. C., and Cruz, C. S. D. (2020). Lung Cancer 2020: Epidemiology, Etiology, and Prevention. *Clin. Chest Med.* 41 (1), 1–24. doi:10.1016/j.ccm.2019.10.001
- Bakhom, S. F., and Cantley, L. C. (2018). The Multifaceted Role of Chromosomal Instability in Cancer and its Microenvironment. *Cell* 174 (6), 1347–1360. doi:10.1016/j.cell.2018.08.027

- Bakhom, S. F., Danilova, O. V., Kaur, P., Levy, N. B., and Compton, D. A. (2011). Chromosomal Instability Substantiates Poor Prognosis in Patients with Diffuse Large B-Cell Lymphoma. *Clin. Cancer Res.* 17 (24), 7704–7711. doi:10.1158/1078-0432.ccr-11-2049
- Bakhom, S. F., Ngo, B., Laughney, A. M., Cavallo, J.-A., Murphy, C. J., Ly, P., et al. (2018). Chromosomal Instability Drives Metastasis through a Cytosolic DNA Response. *Nature* 553 (7689), 467–472. doi:10.1038/nature25432
- Barrett, T., Wilhite, S. E., Ledoux, P., Evangelista, C., Kim, I. F., Tomashevsky, M., et al. (2013). NCBI GEO: Archive for Functional Genomics Data Sets-Uupdate. *Nucleic Acids Res.* 41 (Database issue), D991–D995. doi:10.1093/nar/gks1193
- Ben-David, U., and Amon, A. (2020). Context Is Everything: Aneuploidy in Cancer. *Nat. Rev. Genet.* 21 (1), 44–62. doi:10.1038/s41576-019-0171-x
- Bertran-Alamillo, J., Cattán, V., Schoumacher, M., Codony-Servat, J., Giménez-Capitán, A., Cantero, F., et al. (2019). AURKB as a Target in Non-small Cell Lung Cancer with Acquired Resistance to Anti-EGFR Therapy. *Nat. Commun.* 10 (1), 1812. doi:10.1038/s41467-019-09734-5
- Bild, A. H., Yao, G., Chang, J. T., Wang, Q., Potti, A., Chasse, D., et al. (2006). Oncogenic Pathway Signatures in Human Cancers as a Guide to Targeted Therapies. *Nature* 439 (7074), 353–357. doi:10.1038/nature04296
- Bolhaqueiro, A. C. F., Ponsioen, B., Bakker, B., Klaasen, S. J., Kucukkose, E., van Jaarsveld, R. H., et al. (2019). Ongoing Chromosomal Instability and Karyotype Evolution in Human Colorectal Cancer Organoids. *Nat. Genet.* 51 (5), 824–834. doi:10.1038/s41588-019-0399-6
- Branchi, V., García, S. A., Radhakrishnan, P., Györfy, B., Hissa, B., Schneider, M., et al. (2019). Prognostic Value of DLGAP5 in Colorectal Cancer. *Int. J. Colorectal Dis.* 34 (8), 1455–1465. doi:10.1007/s00384-019-03339-6
- Chen, H., Lee, J., Kljavin, N. M., Haley, B., Daemen, A., Johnson, L., et al. (2015). Requirement for BUB1B/BUBR1 in Tumor Progression of Lung Adenocarcinoma. *Genes. Cancer* 6 (3-4), 106–118. doi:10.18632/genesandcancer.53
- Chen, S., Wang, J., Wang, L., Peng, H., Xiao, L., Li, C., et al. (2019). Silencing TTK Expression Inhibits the Proliferation and Progression of Prostate Cancer. *Exp. Cell Res.* 385 (1), 111669. doi:10.1016/j.yexcr.2019.111669
- Chen, T., Huang, H., Zhou, Y., Geng, L., Shen, T., Yin, S., et al. (2018). HJURP Promotes Hepatocellular Carcinoma Proliferation by Destabilizing P21 via the MAPK/ERK1/2 and AKT/GSK3 $\beta$  Signaling Pathways. *J. Exp. Clin. Cancer Res.* 37 (1), 193. doi:10.1186/s13046-018-0866-4
- Chen, Z., Chai, Y., Zhao, T., Li, P., Zhao, L., He, F., et al. (2019). Effect of PLK1 Inhibition on Cisplatin-resistant Gastric Cancer Cells. *J. Cell. Physiology* 234 (5), 5904–5914. doi:10.1002/jcp.26777
- Chin, C. H., Chen, S. H., Wu, H. H., Ho, C. W., Ko, M. T., and Lin, C. Y. (2014). cytoHubba: Identifying Hub Objects and Sub-networks from Complex Interactome. *BMC Syst. Biol.* 8 (Suppl. 4), S11. doi:10.1186/1752-0509-8-S4-S11
- Chow, M. J., Gu, Y., He, L., Lin, X., Dong, Y., Mei, W., et al. (2021). Prognostic and Therapeutic Potential of the OIP5 Network in Papillary Renal Cell Carcinoma. *Cancers (Basel)* 13 (17), 4483. doi:10.3390/cancers13174483
- Dagogo-Jack, I., and Shaw, A. T. (2018). Tumour Heterogeneity and Resistance to Cancer Therapies. *Nat. Rev. Clin. Oncol.* 15 (2), 81–94. doi:10.1038/nrclinonc.2017.166
- Der, S. D., Sykes, J., Pintilie, M., Zhu, C.-Q., Strumpf, D., Liu, N., et al. (2014). Validation of a Histology-independent Prognostic Gene Signature for Early-Stage, Non-small-cell Lung Cancer Including Stage IA Patients. *J. Thorac. Oncol.* 9 (1), 59–64. doi:10.1097/jto.0000000000000042
- Dhatchinamoorthy, K., Colbert, J. D., and Rock, K. L. (2021). Cancer Immune Evasion through Loss of MHC Class I Antigen Presentation. *Front. Immunol.* 12, 636568. doi:10.3389/fimmu.2021.636568
- Dürbaum, M., and Storchová, Z. (2016). Effects of Aneuploidy on Gene Expression: Implications for Cancer. *FEBS J.* 283 (5), 791–802. doi:10.1111/febs.13591
- Feng, Y., Li, F., Yan, J., Guo, X., Wang, F., Shi, H., et al. (2021). Pan-cancer Analysis and Experiments with Cell Lines Reveal that the Slightly Elevated Expression of DLGAP5 Is Involved in Clear Cell Renal Cell Carcinoma Progression. *Life Sci.* 287, 120056. doi:10.1016/j.lfs.2021.120056
- Feng, Z., Zhang, J., Zheng, Y., Liu, J., Duan, T., and Tian, T. (2021). Overexpression of Abnormal Spindle-like Microcephaly-Associated (ASPM) Increases Tumor Aggressiveness and Predicts Poor Outcome in Patients with Lung Adenocarcinoma. *Transl. Cancer Res. TCR* 10 (2), 983–997. doi:10.21037/ter-20-2570
- Finetti, P., Guille, A., Adelaide, J., Birnbaum, D., Chaffanet, M., and Bertucci, F. (2014). ESPL1 Is a Candidate Oncogene of Luminal B Breast Cancers. *Breast Cancer Res. Treat.* 147 (1), 51–59. doi:10.1007/s10549-014-3070-z
- Fu, J., Li, K., Zhang, W., Wan, C., Zhang, J., Jiang, P., et al. (2020). Large-scale Public Data Reuse to Model Immunotherapy Response and Resistance. *Genome Med.* 12 (1), 21. doi:10.1186/s13073-020-0721-z
- Gan, H., Lin, L., Hu, N., Yang, Y., Gao, Y., Pei, Y., et al. (2019). KIF2C Exerts an Oncogenic Role in Non-small Cell Lung Cancer and Is Negatively Regulated by miR-325-3p. *Cell Biochem. Funct.* 37 (6), 424–431. doi:10.1002/cbf.3420
- Gao, Y., Kim, S., Lee, Y. I., and Lee, J. (2019). Cellular Stress-Modulating Drugs Can Potentially Be Identified by In Silico Screening with Connectivity Map (CMap). *Int. J. Mol. Sci.* 20 (22), 5601. doi:10.3390/ijms20225601
- Gasca, J., Flores, M. L., Giráldez, S., Ruiz-Borrego, M., Tortolero, M., Romero, F., et al. (2016). Loss of FBXW7 and Accumulation of MCL1 and PLK1 Promote Paclitaxel Resistance in Breast Cancer. *Oncotarget* 7 (33), 52751–52765. doi:10.18632/oncotarget.10481
- Gheghiani, L., Wang, L., Zhang, Y., Moore, X. T. R., Zhang, J., Smith, S. C., et al. (2021). PLK1 Induces Chromosomal Instability and Overrides Cell-Cycle Checkpoints to Drive Tumorigenesis. *Cancer Res.* 81 (5), 1293–1307. doi:10.1158/0008-5472.can-20-1377
- Gisselsson, D. (2008). Classification of Chromosome Segregation Errors in Cancer. *Chromosoma* 117 (6), 511–519. doi:10.1007/s00412-008-0169-1
- Gutteridge, R. E. A., Ndiaye, M. A., Liu, X., and Ahmad, N. (2016). Plk1 Inhibitors in Cancer Therapy: From Laboratory to Clinics. *Mol. Cancer Ther.* 15 (7), 1427–1435. doi:10.1158/1535-7163.mct-15-0897
- Hanahan, D., and Weinberg, R. A. (2011). Hallmarks of Cancer: The Next Generation. *Cell* 144 (5), 646–674. doi:10.1016/j.cell.2011.02.013
- He, L., Chen, J., Xu, F., Li, J., and Li, J. (2020). Prognostic Implication of a Metabolism-Associated Gene Signature in Lung Adenocarcinoma. *Mol. Ther. - Oncolytics* 19, 265–277. doi:10.1016/j.omto.2020.09.011
- Herbst, R. S., Morgensztern, D., and Boshoff, C. (2018). The Biology and Management of Non-small Cell Lung Cancer. *Nature* 553 (7689), 446–454. doi:10.1038/nature25183
- Hu, C., Wu, J., Wang, L., Liu, X., Da, B., Liu, Y., et al. (2021). miR-133b Inhibits Cell Proliferation, Migration, and Invasion of Lung Adenocarcinoma by Targeting CDCA8. *Pathology - Res. Pract.* 223, 153459. doi:10.1016/j.prp.2021.153459
- Huang, H., Yang, Y., Zhang, W., Liu, X., and Yang, G. (2020). TTK Regulates Proliferation and Apoptosis of Gastric Cancer Cells through the Akt-mTOR Pathway. *FEBS Open Bio* 10 (8), 1542–1549. doi:10.1002/2211-5463.12909
- Huang, J., Li, Y., Lu, Z., Che, Y., Sun, S., Mao, S., et al. (2019). Analysis of Functional Hub Genes Identifies CDC45 as an Oncogene in Non-small Cell Lung Cancer - a Short Report. *Cell Oncol.* 42 (4), 571–578. doi:10.1007/s13402-019-00438-y
- Huang, Y., Zhong, L., Nie, K., Li, L., Song, S., Liu, F., et al. (2021). Identification of LINC00665-miR-Let-7b-CCNA2 Competing Endogenous RNA Network Associated with Prognosis of Lung Adenocarcinoma. *Sci. Rep.* 11 (1), 4434. doi:10.1038/s41598-020-80662-x
- Hutchinson, B. D., Shroff, G. S., Truong, M. T., and Ko, J. P. (2019). Spectrum of Lung Adenocarcinoma. *Seminars Ultrasound, CT MRI* 40 (3), 255–264. doi:10.1053/j.sult.2018.11.009
- Iwai, Y., Ishida, M., Tanaka, Y., Okazaki, T., Honjo, T., and Minato, N. (2002). Involvement of PD-L1 on Tumor Cells in the Escape from Host Immune System and Tumor Immunotherapy by PD-L1 Blockade. *Proc. Natl. Acad. Sci. U.S.A.* 99 (19), 12293–12297. doi:10.1073/pnas.192461099
- Janssen, A., van der Burg, M., Szuhai, K., Kops, G. J. P. L., and Medema, R. H. (2011). Chromosome Segregation Errors as a Cause of DNA Damage and Structural Chromosome Aberrations. *Science* 333 (6051), 1895–1898. doi:10.1126/science.1210214
- Jiang, J., Liu, T., He, X., Ma, W., Wang, J., Zhou, Q., et al. (2021). Silencing of KIF18B Restricts Proliferation and Invasion and Enhances the Chemosensitivity of Breast Cancer via Modulating Akt/GSK-3 $\beta$ /catenin Pathway. *Biofactors* 47 (5), 754–767. doi:10.1002/biof.1757
- Jiang, X., Jiang, Y., Luo, S., Sekar, K., Koh, C. K. T., Deivasigamani, A., et al. (2021). Correlation of NUF2 Overexpression with Poorer Patient Survival in Multiple Cancers. *Cancer Res. Treat.* 53 (4), 944–961. doi:10.4143/crt.2020.466
- Jin, C.-Y., Du, L., Nuerlan, A.-H., Wang, X.-L., Yang, Y.-W., and Guo, R. (2020). High Expression of RRM2 as an Independent Predictive Factor of Poor Prognosis in Patients with Lung Adenocarcinoma. *Aging* 13 (3), 3518–3535. doi:10.18632/aging.202292

- Kawakami, M., Liu, X., and Dmitrovsky, E. (2019). New Cell Cycle Inhibitors Target Aneuploidy in Cancer Therapy. *Annu. Rev. Pharmacol. Toxicol.* 59, 361–377. doi:10.1146/annurev-pharmtox-010818-021649
- Kimura, S. (2010). AT-9283, a Small-Molecule Multi-Targeted Kinase Inhibitor for the Potential Treatment of Cancer. *Curr. Opin. Investig. Drugs* 11 (12), 1442–1449. doi:10.2174/157015910793358141
- Kou, F., Sun, H., Wu, L., Li, B., Zhang, B., Wang, X., et al. (2020). TOP2A Promotes Lung Adenocarcinoma Cells' Malignant Progression and Predicts Poor Prognosis in Lung Adenocarcinoma. *J. Cancer* 11 (9), 2496–2508. doi:10.7150/jca.41415
- Kou, F., Wu, L., Ren, X., and Yang, L. (2020). Chromosome Abnormalities: New Insights into Their Clinical Significance in Cancer. *Mol. Ther. - Oncolytics* 17, 562–570. doi:10.1016/j.omto.2020.05.010
- Lai, W., Zhu, W., Xiao, C., Li, X., Wang, Y., Han, Y., et al. (2021). HJURP Promotes Proliferation in Prostate Cancer Cells through Increasing CDKN1A Degradation via the GSK3 $\beta$ /JNK Signaling Pathway. *Cell Death Dis.* 12 (6), 583. doi:10.1038/s41419-021-03870-x
- Latchman, Y., Wood, C. R., Chernova, T., Chaudhary, D., Borde, M., Chernova, L., et al. (2001). PD-L2 Is a Second Ligand for PD-1 and Inhibits T Cell Activation. *Nat. Immunol.* 2 (3), 261–268. doi:10.1038/85330
- Lei, Y., Zhang, G., Zhang, C., Xue, L., Yang, Z., Lu, Z., et al. (2021). The Average Copy Number Variation (CNVA) of Chromosome Fragments Is a Potential Surrogate for Tumor Mutational Burden in Predicting Responses to Immunotherapy in Non-small-cell Lung Cancer. *Clin. Transl. Immunol.* 10 (1), e1231. doi:10.1002/cti2.1231
- Levine, M. S., and Holland, A. J. (2018). The Impact of Mitotic Errors on Cell Proliferation and Tumorigenesis. *Genes. Dev.* 32 (9–10), 620–638. doi:10.1101/gad.314351.118
- Li, B., Liu, B., Zhang, X., Liu, H., and He, L. (2020). KIF18B Promotes the Proliferation of Pancreatic Ductal Adenocarcinoma via Activating the Expression of CDCA8. *J. Cell Physiol.* 235 (5), 4227–4238. doi:10.1002/jcp.29201
- Li, J., Wang, R., Schweickert, P. G., Karki, A., Yang, Y., Kong, Y., et al. (2016). Plk1 Inhibition Enhances the Efficacy of Gemcitabine in Human Pancreatic Cancer. *Cell Cycle* 15 (5), 711–719. doi:10.1080/15384101.2016.1148838
- Li, M.-X., Zhang, M.-Y., Dong, H.-H., Li, A.-J., Teng, H.-F., Liu, A.-L., et al. (2021). Overexpression of CENPF Is Associated with Progression and Poor Prognosis of Lung Adenocarcinoma. *Int. J. Med. Sci.* 18 (2), 494–504. doi:10.7150/ijms.49041
- Li, Y., Yi, Q., Liao, X., Han, C., Zheng, L., Li, H., et al. (2021). Hypomethylation-driven Overexpression of HJURP Promotes Progression of Hepatocellular Carcinoma and Is Associated with Poor Prognosis. *Biochem. Biophysical Res. Commun.* 566, 67–74. doi:10.1016/j.bbrc.2021.05.102
- Li, Z., Wang, H., Wei, J., Han, L., and Guo, Z. (2020). Indirubin Exerts Anticancer Effects on Human Glioma Cells by Inducing Apoptosis and Autophagy. *Amb. Expr.* 10 (1), 171. doi:10.1186/s13568-020-01107-2
- Liao, W., Liu, W., Yuan, Q., Liu, X., Ou, Y., He, S., et al. (2013). Silencing of DLGAP5 by siRNA Significantly Inhibits the Proliferation and Invasion of Hepatocellular Carcinoma Cells. *PLoS One* 8 (12), e80789. doi:10.1371/journal.pone.0080789
- Lim, Z.-F., and Ma, P. C. (2019). Emerging Insights of Tumor Heterogeneity and Drug Resistance Mechanisms in Lung Cancer Targeted Therapy. *J. Hematol. Oncol.* 12 (1), 134. doi:10.1186/s13045-019-0818-2
- Lin, W., Chen, Y., Wu, B., Chen, Y., and Li, Z. (2021). Identification of the Pyroptosis-related P-rognostic G-gene S-signature and the A-associated R-regulation axis in L-nug A-denocarcinoma. *Cell Death Discov.* 7 (1), 161. doi:10.1038/s41420-021-00557-2
- Liu, W., Yu, Z., Tang, H., Wang, X., Zhang, B., Zhao, J., et al. (2020). Silencing KIF18B Enhances Radiosensitivity: Identification of a Promising Therapeutic Target in Sarcoma. *EBioMedicine* 61, 103056. doi:10.1016/j.ebiom.2020.103056
- Liu, Y., Zhu, K., Guan, X., Xie, S., Wang, Y., Tong, Y., et al. (2021). TTK Is a Potential Therapeutic Target for Cisplatin-Resistant Ovarian Cancer. *J. Ovarian Res.* 14 (1), 128. doi:10.1186/s13048-021-00884-z
- Liu, Z., Lian, X., Zhang, X., Zhu, Y., Zhang, W., Wang, J., et al. (2021). ESPL1 Is a Novel Prognostic Biomarker Associated with the Malignant Features of Glioma. *Front. Genet.* 12, 666106. doi:10.3389/fgene.2021.666106
- Liu, Z., Sun, Q., and Wang, X. (2017). PLK1, A Potential Target for Cancer Therapy. *Transl. Oncol.* 10 (1), 22–32. doi:10.1016/j.tranon.2016.10.003
- Loeper, S., Romeike, B. F., Heckmann, N., Jung, V., Henn, W., Feiden, W., et al. (2001). Frequent Mitotic Errors in Tumor Cells of Genetically Microheterogeneous Glioblastomas. *Cytogenet. Cell Genet.* 94 (1–2), 1–8. doi:10.1159/000048773
- Love, M. I., Huber, W., and Anders, S. (2014). Moderated Estimation of Fold Change and Dispersion for RNA-Seq Data with DESeq2. *Genome Biol.* 15 (12), 550. doi:10.1186/s13059-014-0550-8
- M'Kacher, R., Andreoletti, L., Flamant, S., Milliat, F., Girinsky, T., Dossou, J., et al. (2010). JC Human Polyomavirus Is Associated to Chromosomal Instability in Peripheral Blood Lymphocytes of Hodgkin's Lymphoma Patients and Poor Clinical Outcome. *Ann. Oncol.* 21 (4), 826–832. doi:10.1093/annonc/mdp375
- Mao, Y., Xi, L., Li, Q., Wang, S., Cai, Z., Zhang, X., et al. (2018). Combination of PI3K/Akt Pathway Inhibition and Plk1 Depletion Can Enhance Chemosensitivity to Gemcitabine in Pancreatic Carcinoma. *Transl. Oncol.* 11 (4), 852–863. doi:10.1016/j.tranon.2018.04.011
- Merino, D. M., McShane, L. M., Fabrizio, D., Funari, V., Chen, S. J., White, J. R., et al. (2020). Establishing Guidelines to Harmonize Tumor Mutational Burden (TMB): In Silico Assessment of Variation in TMB Quantification across Diagnostic Platforms: Phase I of the Friends of Cancer Research TMB Harmonization Project. *J. Immunother. Cancer* 8 (1), e000147. doi:10.1136/jitc-2019-000147
- Mittal, B., Tulsyan, S., Kumar, S., Mittal, R. D., and Agarwal, G. (2015). Cytochrome P450 in Cancer Susceptibility and Treatment. *Adv. Clin. Chem.* 71, 77–139. doi:10.1016/bs.acc.2015.06.003
- Montaudon, E., Nikitorowicz-Buniak, J., Sourd, L., Morisset, L., El Botty, R., Huguët, L., et al. (2020). PLK1 Inhibition Exhibits Strong Anti-tumoral Activity in CCND1-Driven Breast Cancer Metastases with Acquired Palbociclib Resistance. *Nat. Commun.* 11 (1), 4053. doi:10.1038/s41467-020-17697-1
- Moreira, A. L., and Eng, J. (2014). Personalized Therapy for Lung Cancer. *Chest* 146 (6), 1649–1657. doi:10.1378/chest.14-0713
- Naylor, R. M., and van Deursen, J. M. (2016). Aneuploidy in Cancer and Aging. *Annu. Rev. Genet.* 50, 45–66. doi:10.1146/annurev-genet-120215-035303
- Neumüller, R. A., and Knoblich, J. A. (2009). Dividing Cellular Asymmetry: Asymmetric Cell Division and its Implications for Stem Cells and Cancer. *Genes. Dev.* 23 (23), 2675–2699. doi:10.1101/gad.1850809
- Newman, A. M., Liu, C. L., Green, M. R., Gentles, A. J., Feng, W., Xu, Y., et al. (2015). Robust Enumeration of Cell Subsets from Tissue Expression Profiles. *Nat. Methods* 12 (5), 453–457. doi:10.1038/nmeth.3337
- Ninomiya, H., Nomura, K., Satoh, Y., Okumura, S., Nakagawa, K., Fujiwara, M., et al. (2006). Genetic Instability in Lung Cancer: Concurrent Analysis of Chromosomal, Mini- and Microsatellite Instability and Loss of Heterozygosity. *Br. J. Cancer* 94 (10), 1485–1491. doi:10.1038/sj.bjc.6603121
- Nooreldeen, R., and Bach, H. (2021). Current and Future Development in Lung Cancer Diagnosis. *Int. J. Mol. Sci.* 22 (16), 8661. doi:10.3390/ijms22168661
- Ogata, H., Goto, S., Sato, K., Fujibuchi, W., Bono, H., and Kanehisa, M. (1999). KEGG: Kyoto Encyclopedia of Genes and Genomes. *Nucleic Acids Res.* 27 (1), 29–34. doi:10.1093/nar/27.1.29
- Peng, B., Shi, R., Bian, J., Li, Y., Wang, P., Wang, H., et al. (2021). PARP1 and CHK1 Coordinate PLK1 Enzymatic Activity during the DNA Damage Response to Promote Homologous Recombination-Mediated Repair. *Nucleic Acids Res.* 49 (13), 7554–7570. doi:10.1093/nar/gkab584
- Philpott, C., Tovell, H., Frayling, I. M., Cooper, D. N., and Upadhyaya, M. (2017). The NF1 Somatic Mutational Landscape in Sporadic Human Cancers. *Hum. Genomics* 11 (1), 13. doi:10.1186/s40246-017-0109-3
- Potapova, T., and Gorbsky, G. J. (2017). The Consequences of Chromosome Segregation Errors in Mitosis and Meiosis. *Biol. (Basel)* 6 (1), 12. doi:10.3390/biology6010012
- Puhr, H. C., and Ilhan-Mutlu, A. (2019). New Emerging Targets in Cancer Immunotherapy: The Role of LAG3. *ESMO Open* 4 (2), e000482. doi:10.1136/esmoopen-2018-000482
- Qi, G., Ma, H., Li, Y., Peng, J., Chen, J., and Kong, B. (2021). TTK Inhibition Increases Cisplatin Sensitivity in High-Grade Serous Ovarian Carcinoma through the mTOR/autophagy Pathway. *Cell Death Dis.* 12 (12), 1135. doi:10.1038/s41419-021-04429-6
- Ramani, P., Nash, R., Sowa-Avugrah, E., and Rogers, C. (2015). High Levels of Polo-like Kinase 1 and Phosphorylated Translationally Controlled Tumor

- Protein Indicate Poor Prognosis in Neuroblastomas. *J. Neurooncol* 125 (1), 103–111. doi:10.1007/s11060-015-1900-4
- Reisländer, T., Groelly, F. J., and Tarsounas, M. (2020). DNA Damage and Cancer Immunotherapy: A STING in the Tale. *Mol. Cell* 80 (1), 21–28. doi:10.1016/j.molcel.2020.07.026
- Rodrigues-Junior, D. M., Biassi, T. P., Carlin, V., Buri, M. V., Torrecilhas, A. C., Bortoluci, K. R., et al. (2018). OIP5 Expression Sensitize Glioblastoma Cells to Lumustine Treatment. *J. Mol. Neurosci.* 66 (3), 383–389. doi:10.1007/s12031-018-1184-1
- Rousseaux, S., Debernardi, A., Jacquiau, B., Vitte, A. L., Vesin, A., Nagy-Mignotte, H., et al. (2013). Ectopic Activation of Germline and Placental Genes Identifies Aggressive Metastasis-Prone Lung Cancers. *Sci. Transl. Med.* 5 (186), 186ra66. doi:10.1126/scitranslmed.3005723
- Sarkar, S., Sahoo, P. K., Mahata, S., Pal, R., Ghosh, D., Mistry, T., et al. (2021). Mitotic checkpoint defects: En route to cancer and drug resistance. *Chromosome Res.* 29 (2), 131–144. doi:10.1007/s10577-020-09646-x
- Schneider, M. A., Christopoulos, P., Muley, T., Warth, A., Klingmueller, U., Thomas, M., et al. (2017). AURKA, DLGAP5, TPX2, KIF11 and CKAP5: Five Specific Mitosis-Associated Genes Correlate with Poor Prognosis for Non-small Cell Lung Cancer Patients. *Int. J. Oncol.* 50 (2), 365–372. doi:10.3892/ijo.2017.3834
- Serafim, R. B., Cardoso, C., Di Cristofaro, L. F. M., Soares, C. P., Silva, W. A., Espreefco, E. M., et al. (2020). HJURP Knockdown Disrupts Clonogenic Capacity and Increases Radiation-Induced Cell Death of Glioblastoma Cells. *Cancer Gene Ther.* 27 (5), 319–329. doi:10.1038/s41417-019-0103-0
- Shan, L., Zhu, X.-L., Zhang, Y., Gu, G.-J., and Cheng, X. (2021). Expression and Clinical Significance of NUF2 in Kidney Renal Clear Cell Carcinoma. *Transl. Androl. Urol.* 10 (9), 3628–3637. doi:10.21037/tau-21-620
- Shannon, P., Markiel, A., Ozier, O., Baliga, N. S., Wang, J. T., Ramage, D., et al. (2003). Cytoscape: A Software Environment for Integrated Models of Biomolecular Interaction Networks. *Genome Res.* 13 (11), 2498–2504. doi:10.1101/gr.1239303
- Shao, C., Ahmad, N., Hodges, K., Kuang, S., Ratliff, T., and Liu, X. (2015). Inhibition of Polo-like Kinase 1 (Plk1) Enhances the Antineoplastic Activity of Metformin in Prostate Cancer. *J. Biol. Chem.* 290 (4), 2024–2033. doi:10.1074/jbc.m114.596817
- Shapouri-Moghaddam, A., Mohammadian, S., Vazini, H., Taghadosi, M., Esmaili, S. A., Mardani, F., et al. (2018). Macrophage Plasticity, Polarization, and Function in Health and Disease. *J. Cell Physiol.* 233 (9), 6425–6440. doi:10.1002/jcp.26429
- Shin, S. B., Kim, C. H., Jang, H. R., and Yim, H. (2020). Combination of Inhibitors of USP7 and PLK1 Has a Strong Synergism against Paclitaxel Resistance. *Int. J. Mol. Sci.* 21 (22), 8629. doi:10.3390/ijms21228629
- Shin, S. B., Woo, S. U., and Yim, H. (2019). Cotargeting Plk1 and Androgen Receptor Enhances the Therapeutic Sensitivity of Paclitaxel-Resistant Prostate Cancer. *Ther. Adv. Med. Oncol.* 11, 1758835919846375. doi:10.1177/1758835919846375
- Singel, S. M., Cornelius, C., Zaganjor, E., Batten, K., Sarode, V. R., Buckley, D. L., et al. (2014). KIF14 Promotes AKT Phosphorylation and Contributes to Chemoresistance in Triple-Negative Breast Cancer. *Neoplasia* 16 (3), 247–256. doi:10.1016/j.neo.2014.03.008
- Solinas, C., Migliori, E., De Silva, P., and Willard-Gallo, K. (2019). LAG3: The Biological Processes that Motivate Targeting This Immune Checkpoint Molecule in Human Cancer. *Cancers (Basel)* 11 (8), 1213. doi:10.3390/cancers11081213
- Song, B., Liu, X. S., Rice, S. J., Kuang, S., Elzey, B. D., Konieczny, S. F., et al. (2013). Plk1 Phosphorylation of Orc2 and Hbo1 Contributes to Gemcitabine Resistance in Pancreatic Cancer. *Mol. Cancer Ther.* 12 (1), 58–68. doi:10.1158/1535-7163.mct-12-0632
- Song, J., Sun, Y., Cao, H., Liu, Z., Xi, L., Dong, C., et al. (2021). A Novel Pyroptosis-Related lncRNA Signature for Prognostic Prediction in Patients with Lung Adenocarcinoma. *Bioengineered* 12 (1), 5932–5949. doi:10.1080/21655979.2021.1972078
- Soto, M., Raaijmakers, J. A., and Medema, R. H. (2019). Consequences of Genomic Diversification Induced by Segregation Errors. *Trends Genet.* 35 (4), 279–291. doi:10.1016/j.tig.2019.01.003
- Sturm, G., Finotello, F., and List, M. (2020). Immunedeconv: An R Package for Unified Access to Computational Methods for Estimating Immune Cell Fractions from Bulk RNA-Sequencing Data. *Methods Mol. Biol.* 2120, 223–232. doi:10.1007/978-1-0716-0327-7\_16
- Sun, G. Z., and Zhao, T. W. (2019). Lung Adenocarcinoma Pathology Stages Related Gene Identification. *Math. Biosci. Eng.* 17 (1), 737–746. doi:10.3934/mbe.2020038
- Sun, S., Guo, W., Wang, Z., Wang, X., Zhang, G., Zhang, H., et al. (2020). Development and Validation of an Immune-related Prognostic Signature in Lung Adenocarcinoma. *Cancer Med.* 9 (16), 5960–5975. doi:10.1002/cam4.3240
- Szklarczyk, D., Gable, A. L., Lyon, D., Junge, A., Wyder, S., Huerta-Cepas, J., et al. (2019). STRING V11: Protein-Protein Association Networks with Increased Coverage, Supporting Functional Discovery in Genome-wide Experimental Datasets. *Nucleic Acids Res.* 47 (D1), D607–D613. doi:10.1093/nar/gky1131
- Tanaka, K., and Hirota, T. (2009). Chromosome Segregation Machinery and Cancer. *Cancer Sci.* 100 (7), 1158–1165. doi:10.1111/j.1349-7006.2009.01178.x
- Tayoun, T., Oulhen, M., Aberlenc, A., Farace, F., and Pawlikowska, P. (2021). Tumor Evolution and Therapeutic Choice Seen through a Prism of Circulating Tumor Cell Genomic Instability. *Cells* 10 (2), 337. doi:10.3390/cells10020337
- Testa, D., Jourde-Chiche, N., Mancini, J., Varriale, P., Radoszycki, L., and Chiche, L. (2021). Unsupervised Clustering Analysis of Data from an Online Community to Identify Lupus Patient Profiles with Regards to Treatment Preferences. *Lupus* 30 (11), 1837–1843. doi:10.1177/09612033211033977
- Tomczak, K., Czerwińska, P., and Wiznerowicz, M. (2015). The Cancer Genome Atlas (TCGA): An Immeasurable Source of Knowledge. *Contemp. Oncol. Pozn.* 19 (1A), A68–A77. doi:10.5114/wo.2014.47136
- Tomida, S., Takeuchi, T., Shimada, Y., Arima, C., Matsuo, K., Mitsudomi, T., et al. (2009). Relapse-related Molecular Signature in Lung Adenocarcinomas Identifies Patients with Dismal Prognosis. *J. Clin. Oncol.* 27 (17), 2793–2799. doi:10.1200/jco.2008.19.7053
- Torre, L. A., Siegel, R. L., and Jemal, A. (2016). Lung Cancer Statistics. *Adv. Exp. Med. Biol.* 893, 1–19. doi:10.1007/978-3-319-24223-1\_1
- Travis, W. D., Brambilla, E., Noguchi, M., Nicholson, A. G., Geisinger, K., Yatabe, Y., et al. (2011). International Association for the Study of Lung Cancer/American Thoracic Society/European Respiratory Society: International Multidisciplinary Classification of Lung Adenocarcinoma: Executive Summary. *Proc. Am. Thorac. Soc.* 8 (5), 381–385. doi:10.1513/pats.201107-042st
- Tut, T. G., Lim, S. H. S., Dissanayake, I. U., Descallar, J., Chua, W., Ng, W., et al. (2015). Upregulated Polo-Like Kinase 1 Expression Correlates with Inferior Survival Outcomes in Rectal Cancer. *PLoS One* 10 (6), e0129313. doi:10.1371/journal.pone.0129313
- Wang, L., Yang, X., An, N., and Liu, J. (2020). Bioinformatics Analysis of BUB1 Expression and Gene Regulation Network in Lung Adenocarcinoma. *Transl. Cancer Res. TCR* 9 (8), 4820–4833. doi:10.21037/tcr-20-1045
- Wang, M., Du, Q., Jin, J., Wei, Y., Lu, Y., and Li, Q. (2021). LAG3 and its Emerging Role in Cancer Immunotherapy. *Clin. Transl. Med.* 11 (3), e365. doi:10.1002/ctm2.365
- Wang, P., Yu, N., Wang, Y., Sun, H., Yang, Z., and Zhou, S. (2018). Co-delivery of PLK1-specific shRNA and Doxorubicin via Core-Crosslinked pH-Sensitive and Redox Ultra-sensitive Micelles for Glioma Therapy. *J. Mat. Chem. B* 6 (1), 112–124. doi:10.1039/c7tb02160g
- Wang, R., Zang, W., Hu, B., Deng, D., Ling, X., Zhou, H., et al. (2020). Serum ESPL1 Can Be Used as a Biomarker for Patients with Hepatitis B Virus-Related Liver Cancer: A Chinese Case-Control Study. *Technol. Cancer Res. Treat.* 19, 1533033820980785. doi:10.1177/1533033820980785
- Wang, S., Sun, H., Zhan, X., and Wang, Q. (2021). [Retracted] MicroRNA718 Serves a Tumorsuppressive Role in Nonsmall Cell Lung Cancer by Directly Targeting CCNB1. *Int. J. Mol. Med.* 48 (3), 180. doi:10.3892/ijmm.2021.5013
- Wang, X., Xiao, H., Wu, D., Zhang, D., and Zhang, Z. (2020). miR-335-5p Regulates Cell Cycle and Metastasis in Lung Adenocarcinoma by Targeting CCNB2. *Onco. Targets Ther.* 13, 6255–6263. doi:10.2147/ott.s245136
- Wang, Z. Z., Yang, J., Jiang, B. H., Di, J. B., Gao, P., Peng, L., et al. (2018). KIF14 Promotes Cell Proliferation via Activation of Akt and Is Directly Targeted by miR-200c in Colorectal Cancer. *Int. J. Oncol.* 53 (5), 1939–1952. doi:10.3892/ijo.2018.4546
- Wei, Y., Ouyang, G. L., Yao, W. X., Zhu, Y. J., Li, X., Huang, L. X., et al. (2019). Knockdown of HJURP Inhibits Non-small Cell Lung Cancer Cell

- Proliferation, Migration, and Invasion by Repressing Wnt/ $\beta$ -Catenin Signaling. *Eur. Rev. Med. Pharmacol. Sci.* 23 (9), 3847–3856. doi:10.26355/eurrev\_201905\_17812
- Wilkerson, M. D., and Hayes, D. N. (2010). ConsensusClusterPlus: A Class Discovery Tool with Confidence Assessments and Item Tracking. *Bioinformatics* 26 (12), 1572–1573. doi:10.1093/bioinformatics/btq170
- Wu, Y., Lin, Y., Pan, J., Tu, X., Xu, Y., Li, H., et al. (2021). NCAPG Promotes the Progression of Lung Adenocarcinoma via the TGF- $\beta$  Signaling Pathway. *Cancer Cell Int.* 21 (1), 443. doi:10.1186/s12935-021-02138-w
- Xia, Y., Rao, L., Yao, H., Wang, Z., Ning, P., and Chen, X. (2020). Engineering Macrophages for Cancer Immunotherapy and Drug Delivery. *Adv. Mater.* 32 (40), e2002054. doi:10.1002/adma.202002054
- Xiao, L., Zhang, S., Zheng, Q., and Zhang, S. (2021). Dysregulation of KIF14 Regulates the Cell Cycle and Predicts Poor Prognosis in Cervical Cancer: A Study Based on Integrated Approaches. *Braz J. Med. Biol. Res.* 54 (11), e11363. doi:10.1590/1414-431X2021e11363
- Xie, X., Jiang, S., and Li, X. (2021). Nuf2 Is a Prognostic-Related Biomarker and Correlated with Immune Infiltrates in Hepatocellular Carcinoma. *Front. Oncol.* 11, 621373. doi:10.3389/fonc.2021.621373
- Xu, R., Zhang, Y., Li, A., Ma, Y., Cai, W., Song, L., et al. (2021). LY-294002 Enhances the Chemosensitivity of Liver Cancer to Oxaliplatin by Blocking the PI3K/AKT/HIF-1 $\alpha$  Pathway. *Mol. Med. Rep.* 24 (1), 508. doi:10.3892/mmr.2021.12147
- Xu, T., Dong, M., Li, H., Zhang, R., and Li, X. (2020). Elevated mRNA Expression Levels of DLGAP5 Are Associated with Poor Prognosis in Breast Cancer. *Oncol. Lett.* 19 (6), 4053–4065. doi:10.3892/ol.2020.11533
- Yamauchi, M., Yamaguchi, R., Nakata, A., Kohno, T., Nagasaki, M., Shimamura, T., et al. (2012). Epidermal Growth Factor Receptor Tyrosine Kinase Defines Critical Prognostic Genes of Stage I Lung Adenocarcinoma. *PLoS One* 7 (9), e43923. doi:10.1371/journal.pone.0043923
- Yoshihara, K., Shahmoradgoli, M., Martínez, E., Vegesna, R., Kim, H., Torres-García, W., et al. (2013). Inferring Tumour Purity and Stromal and Immune Cell Admixture from Expression Data. *Nat. Commun.* 4, 2612. doi:10.1038/ncomms3612
- Yu, G., Wang, L.-G., Han, Y., and He, Q.-Y. (2012). clusterProfiler: An R Package for Comparing Biological Themes Among Gene Clusters. *OMICS A J. Integr. Biol.* 16 (5), 284–287. doi:10.1089/omi.2011.0118
- Zhang, H., Liu, Y., Tang, S., Qin, X., Li, L., Zhou, J., et al. (2021). Knockdown of DLGAP5 Suppresses Cell Proliferation, Induces G2/M Phase Arrest and Apoptosis in Ovarian Cancer. *Exp. Ther. Med.* 22 (5), 1245. doi:10.3892/etm.2021.10680
- Zhang, H., Yao, W., Zhang, M., Lu, Y., Tang, J., Jiang, M., et al. (2021). TTK Inhibitor Promotes Radiosensitivity of Liver Cancer Cells through P21. *Biochem. Biophysical Res. Commun.* 550, 84–91. doi:10.1016/j.bbrc.2021.01.089
- Zhang, R., Shi, H., Ren, F., Liu, H., Zhang, M., Deng, Y., et al. (2015). Misregulation of Polo-like Protein Kinase 1, P53 and P21WAF1 in Epithelial Ovarian Cancer Suggests Poor Prognosis. *Oncol. Rep.* 33 (3), 1235–1242. doi:10.3892/or.2015.3723
- Zhang, Z., Hou, S.-Q., He, J., Gu, T., Yin, Y., and Shen, W. H. (2016). PTEN Regulates PLK1 and Controls Chromosomal Stability during Cell Division. *Cell Cycle* 15 (18), 2476–2485. doi:10.1080/15384101.2016.1203493
- Zheng, R., Shi, Z., Li, W., Yu, J., Wang, Y., and Zhou, Q. (2020). Identification and Prognostic Value of DLGAP5 in Endometrial Cancer. *PeerJ* 8, e10433. doi:10.7717/peerj.10433
- Zhou, D., Wang, M., Zhang, Y., Wang, K., Zhao, M., Wang, Y., et al. (2021). Screening and Identification of LMNB1 and DLGAP5, Two Key Biomarkers in Gliomas. *Biosci. Rep.* 41 (5), BSR20210231. doi:10.1042/bsr20210231
- Zhou, J., Jiang, G., Xu, E., Zhou, J., Liu, L., and Yang, Q. (2021). Identification of SRXN1 and KRT6A as Key Genes in Smoking-Related Non-small-cell Lung Cancer through Bioinformatics and Functional Analyses. *Front. Oncol.* 11, 810301. doi:10.3389/fonc.2021.810301
- Zhu, D., Xia, J., Liu, C., and Fang, C. (2022). Numb/Notch/PLK1 Signaling Pathway Mediated Hyperglycemic Memory in Pancreatic Cancer Cell Radioresistance and the Therapeutic Effects of Metformin. *Cell. Signal.* 93, 110268. doi:10.1016/j.cellsig.2022.110268

**Conflict of Interest:** The authors declare that the research was conducted in the absence of any commercial or financial relationships that could be construed as a potential conflict of interest.

**Publisher's Note:** All claims expressed in this article are solely those of the authors and do not necessarily represent those of their affiliated organizations, or those of the publisher, the editors, and the reviewers. Any product that may be evaluated in this article, or claim that may be made by its manufacturer, is not guaranteed or endorsed by the publisher.

Copyright © 2022 Li, Ma, Xue, Shen, Qin, Zhang, Zheng and Zhang. This is an open-access article distributed under the terms of the Creative Commons Attribution License (CC BY). The use, distribution or reproduction in other forums is permitted, provided the original author(s) and the copyright owner(s) are credited and that the original publication in this journal is cited, in accordance with accepted academic practice. No use, distribution or reproduction is permitted which does not comply with these terms.